CVJ CLUJ VETERINARY JOURNAL

Table of contents

CVJ CLUJ VETERINARY JOURNAL

Research article

Intramammary bacterial profile and its impact on the number and differential distribution of somatic cells in the context of drying off in dairy cows

Ionela-Delia Uț [1], Daniel Ionuț Berean [1,*], Simona Ciupe [1], Ștefan Coman [1] and Liviu Marian Bogdan [1]

[1] Department of Reproduction, Faculty of Veterinary Medicine, University of Agricultural Sciences and Veterinary Medicine Cluj-Napoca, Calea Mănăştur 3-5, 400372 Cluj-Napoca, Romania
* Correspondence: daniel.berean@usamvcluj.ro

Abstract: Mastitis remains one of the most significant conditions in dairy cattle farms, with major consequences for animal health and milk quality. The aim of this study was to determine the prevalence of intramammary infections (IMI) and to analyze the relationship between the pathogens involved, the total somatic cell count (SCC), and their differential distribution (DSCC) in two family-owned farms of Romanian Spotted cows, evaluated before and after drying-off. A total of 140 milk samples were collected and analyzed using standard microbiological examinations, as well as SCC and DSCC determinations by flow cytometry. The results revealed an overall IMI prevalence of 32.9%, with differences between the two farms: in Farm 1, major pathogens predominated (*Streptococcus agalactiae*, *Streptococcus uberis*, *Streptococcus dysgalactiae*, *Escherichia coli*), whereas in Farm 2, minor pathogens were more frequently isolated (coagulase-negative staphylococci, *Corynebacterium* spp.). The mean SCC value was significantly higher in positive samples (807,557 cells/mL) compared to negative samples (98,243 cells/mL), with the highest values associated with *E. coli* infections. Similarly, DSCC showed marked differences between uninfected (26.2%) and positive samples (68.4%), with a tentative threshold of 65% suggested as indicative of intramammary infection. The results confirm the utility of combining SCC and DSCC for more accurate mastitis detection and highlight the importance of pathogen characterization at the farm level to optimize management strategies and apply selective therapy at drying-off.

Keywords: mastitis; intramammary infection; dairy cows; somatic cell count; differential somatic cell count;

1. Introduction

In the current context of dairy cattle farms, mastitis, defined as inflammation of the mammary gland, remains one of the most significant conditions, with direct effects on both animal health and milk quantity and quality [1]. Considering that the International Dairy Federation (IDF) indicates that the etiology of mastitis is most frequently associated with infectious agents [2], knowledge of the epidemiological situation on farms is essential for rapid diagnosis and informed decision-making regarding udder health management at both herd and individual levels [1]. In the scientific literature, pathogens involved in mastitis are commonly grouped into two major categories: contagious and environmental pathogens, each playing a distinct role in the disease dynamics and its management [3].

The main contagious pathogens include *Staphylococcus aureus, Streptococcus agalactiae*, and *Mycoplasma bovis*, recognized for their ability to cause persistent and difficult-to-eradicate infections. Regarding environmental mastitis, the etiological spectrum is more diverse, with coliforms such as *Escherichia coli, Klebsiella spp*, and *Enterobacter spp*, environmental streptococci such as *Streptococcus uberis* and *Streptococcus dysgalactiae*, and non-aureus staphylococci (NAS) most frequently identified [4]. Most infections caused by these pathogens manifest as clinical mastitis, which is readily detectable on the farm through visible changes in the mammary gland or milk. However, a substantial proportion of cases remain undetected clinically, presenting as subclinical mastitis (SM) [5], which is primarily identified through elevated somatic cell counts (SCC) [2]. Milk SCC reflects the cellular population of the mammary gland and consists mainly of leukocytes,

Received: 01.10.2025
Accepted: 02.12.2025
Published: 27.02.2026

DOI:10.52331/v31i1kv49

including macrophages, neutrophils, and lymphocytes, along with a small proportion of mammary epithelial cells, representing less than 7% of the total [6]. Under normal physiological conditions, the mammary gland maintains a low cell count, internationally considered healthy up to approximately 200,000 cells/mL [2]. Thus, the SCC in an individual cow's milk or bulk milk represents a reliable quantitative indicator of mammary gland inflammation [7,8] and is used worldwide for assessing udder health in lactating animals [9], as well as for guiding selective dry cow therapy (SDCT) [10]. Although several factors can influence SCC variation in lactating cows, such as age, parity, lactation stage, and season, the presence of infection remains the primary determinant of these fluctuations [11].

An essential aspect highlighted by previous research is the correlation between SCC variations and the type of pathogen involved in mastitis. Major pathogens, including *S. aureus*, *S. agalactiae*, coliforms, and other *Streptococcus species* (excluding *S. agalactiae*), are associated with the highest SCC elevations, whereas minor pathogens, such as *Corynebacterium bovis* and coagulase-negative staphylococci (CNS), generally produce only moderate increases in SCC [12–14]. Understanding this dynamic is crucial for developing realistic models to support decision-making regarding treatment and culling, ensuring economic efficiency and optimal udder health management. In recent years, to enhance the sensitivity and accuracy of SCC in identifying mammary inflammation, researchers have introduced an additional parameter for evaluating udder health: the differential somatic cell count (DSCC) [15]. Unlike SCC, which indicates the total cell count in milk, DSCC highlights the proportions of lymphocytes, macrophages, and polymorphonuclear cells directly involved in the defense mechanisms and inflammatory response of the mammary gland [16]. Studies have proposed DSCC thresholds between 56% and 72% [15,17], but have also shown that this parameter varies depending on the pathogen involved [18–20], the stage of mastitis, and parity [21]. Higher DSCC values have been observed in the early phases of intramammary infections (IMI) caused by major pathogens such as environmental streptococci, *S. aureus*, and coliforms [22].

However, the literature still provides limited information on the impact of mastitis on the dynamics of this indicator. Therefore, DSCC is recommended to be used in conjunction with SCC and other farm-level data, with thresholds adapted to specific farm conditions and management strategies [17]. The objectives of this study were to determine the prevalence of IMI caused by different microorganisms in two family-owned Romanian Spotted dairy farms during the drying-off period and immediately thereafter, and to analyze the relationships between microbial agents, total somatic cell counts, and their differential distribution. Obtaining this information aims to provide an epidemiological overview at the farm level, supporting informed decisions regarding udder treatments and management strategies during the drying-off period.

2. Materials and Methods

2.1. Description of the farms and animals included in the study

The study was conducted between November 2024 and June 2025 in two family-owned Romanian Spotted dairy farms located in Cluj County, Romania. Farm 1 included a herd of 63 lactating cows with an average milk production of 26.4 L/cow, while Farm 2 comprised 51 lactating cows with an average milk production of 20.1 L/cow. Both farms operated under similar management conditions. Cows were housed in a free-stall system, with individual resting areas and access to common feeding spaces. The feed ration was comparable between the two farms, consisting of corn silage, alfalfa hay, straw, and protein concentrates with mineral-vitamin supplements, administered as a Total Mixed Ration (TMR). Milking was performed twice daily, in the morning and evening, in parlors equipped with milk hygiene and monitoring systems. In both farms, cows were dried off gradually by progressively reducing the number of milkings, following standard dairy farm practices. Drying off was performed using Blanket Dry Cow Therapy (BDCT), whereby antibiotics were administered to all quarters of all cows, irrespective of their infection status. This standardized approach to housing, feeding, and milking ensured the comparability of data obtained from the herds.

2.2. Sampling protocols before and after drying-off

For this study, 68 cows approaching the dry period were selected, 34 from each farm. Milk samples were collected in the morning, before milking, and included milk from all four udder quarters. Sampling was performed at two distinct time points: 5–10 days before drying-off and 4–7 days after drying-off, except for four cases (two from each farm) that required a third sampling due to the development of clinical mastitis, resulting in a total of 140 milk samples. For each animal, two samples were collected at each time point: one for SCC and DSCC determination, and the other for microbiological analysis. The SCC/DSCC sample was collected using a milkometer, a standardized device that measures milk quantity and composition and

allows a representative sample by proportionally collecting milk from all udder quarters. These samples were placed in sterile tubes without preservatives and transported directly to the laboratory immediately after collection. Microbiological samples were collected under aseptic conditions following the protocol recommended by the National Mastitis Council [23]. Teat preparation included removing dirt and debris by brushing, performing forestripping, and disinfecting each teat with an iodine-based solution (KerbaWasch 2%, Kerbl, Germany) left for 30 seconds. Teats were then dried with individual paper towels. Immediately before sampling, the teat tip and barrel were wiped with sterile gauze soaked in 70% isopropyl alcohol. Samples were collected under hygienic conditions using disposable nitrile gloves. A few streams of milk were manually discarded from each quarter, after which 10–20 mL of milk were collected in sterile plastic containers for standard aerobic bacterial culture. All samples were properly labeled, and container numbers were correlated with each cow's identity. Samples were kept on ice and transported promptly to the laboratory for processing.

2.3. Determination of SCC and DSCC

SCC and DSCC were determined at the Milk Quality Control Foundation laboratory in Cluj-Napoca using the automated Fossomatic™ system (FOSS, Hillerød, Denmark), based on flow cytometry and in accordance with IDF standards. DSCC was determined using the method described by Damm et al. [15], which allows the identification, in a milk sample, of macrophages (MAC) and the combined population of polymorphonuclear leukocytes (PMN) and lymphocytes (LYM). DSCC is expressed as the combined proportion (%) of PMN and LYM relative to the total somatic cells in milk.

2.4. Bacterial Identification

Mastitis pathogens were identified at the Microbiology Laboratory of the Milk Quality Control Foundation, Cluj-Napoca. Milk samples were initially inoculated on chromogenic, selective, and differential media to isolate the main bacteria involved in mastitis: CPS (ChromID® CPS® Elite agar) for detection and differentiation of coliforms and enterococci, and Baird-Parker agar for selective isolation of *S. aureus*. Colonies with low growth or small size on CPS were subsequently transferred to Columbia Blood Agar, a nutrient-rich medium, to allow full bacterial development and observation of morphological characteristics and hemolysis. Plates were incubated aerobically at 37 °C for 18–24 h to obtain isolated colonies. Culture purity was verified through morphological inspection and Gram staining, and representative colonies were selected for identification. Growth of three or more bacterial types was considered a contaminated culture and excluded from analysis. From compliant cultures, bacterial suspensions were prepared in sterile saline (0.45–0.50% NaCl), adjusted to McFarland 0.5 standard (~1.5×10^8 CFU/mL) using the DensiCHEK system (bioMérieux, France). Standardized suspensions were inoculated into VITEK® 2 cards appropriate for Gram-positive or Gram-negative microorganisms and processed automatically in the VITEK® 2 Compact system (bioMérieux, France) according to manufacturer instructions and IDF bacterial identification standards.

2.5. Statistical Analyses

Statistical analyses were performed using Microsoft Excel**.** Descriptive statistics were applied to characterize SCC and DSCC in animals according to mastitis pathogens and infection status. Arithmetic mean, geometric mean, standard deviation, and median were calculated to describe data distribution and highlight variations between different groups.

3. Results

3.1. Microbiological examinations and infection prevalence

A total of 140 samples were analyzed through microbiological examinations, SCC, and DSCC determination. Of these, 94 samples (67.1%) showed no bacterial growth, while 46 samples (32.9%) were positive for at least one mastitis pathogen. Among all samples from animals, 4 (2.9%) were classified as contaminated during microbiological examination, according to the criteria of Harmon et al. [24]. From the milk samples with bacterial growth, the following bacteria were isolated: 21 samples (50%) with CNS, with the most frequent species being *S. chromogenes* (28.81%), *S. epidermidis* (19.05%), *S. simulans* (19.05%), and S. *xylosus* (14.29%), and other species including *S. haemolyticus, S. warneri*, and *S. sciuri.* Additionally, 7 samples (16.67%) were positive for *Streptococcus uberis*, 5 samples (11.90%) for *S. agalactiae*, 3 samples (7.14%) for *S. aureus*, 2 samples (4.76%) for *S. dysgalactiae*, 2 samples (4.76%) for *E. coli*, and 2 samples (4.76%) for *Corynebacterium spp*.

In Farm 1, out of 70 samples, 28 were positive, of which two were excluded due to contamination. From the remaining 26 positive samples (37.14%), 12 samples (46.15%) were infected with minor pathogens, represented by CNS, while 14 samples (53.85%) contained major pathogens, including *S. agalactiae, S. dysgalactiae, S. uberis*, and *E. coli*. Infection prevalence before drying off was 38.24% (13 positive samples out of 34 collected) and after calving was 36.11% (13 positive samples out of 36 collected). The mean SCC before drying off was 482,735 cells/mL, and the mean DSCC was 47.8%. After calving, the mean SCC was 384,176 cells/mL, while the mean DSCC was 42.5%.

In Farm 2, out of 70 samples, 18 were positive, of which two were excluded due to contamination. From the remaining 16 positive samples (22.86%), 11 samples (68.75%) were infected with minor pathogens, represented by CNS *and Corynebacterium spp*., and 5 samples (31.25%) with major pathogens, namely *S. aureus* and *S. uberis*. Infection prevalence before drying off was 29.41% (10 positive samples out of 34 collected), and after calving was 16.67% (6 positive samples out of 36 collected). The mean SCC before drying off was 268,485 cells/mL, and the mean DSCC was 33.88%. After calving, the mean SCC was 270,250 cells/mL, and the mean DSCC was 29.7%.

The results regarding the prevalence of pathogens identified in the two farms are summarized in Figure 1. Overall, total infection prevalence was higher in Farm 1 both before drying off and after calving, as reflected by the greater number of positive samples. In Farm 1, post-calving prevalence remained relatively constant, whereas in Farm 2 it decreased significantly. Moreover, the prevalence of major pathogens was higher in Farm 1 compared to Farm 2, while infections with minor pathogens predominated in Farm 2. CNS and *S. uberis* were commonly isolated from both herds. Additionally, both before and after drying off, the mean SCC and DSCC were higher in Farm 1 compared to Farm 2.

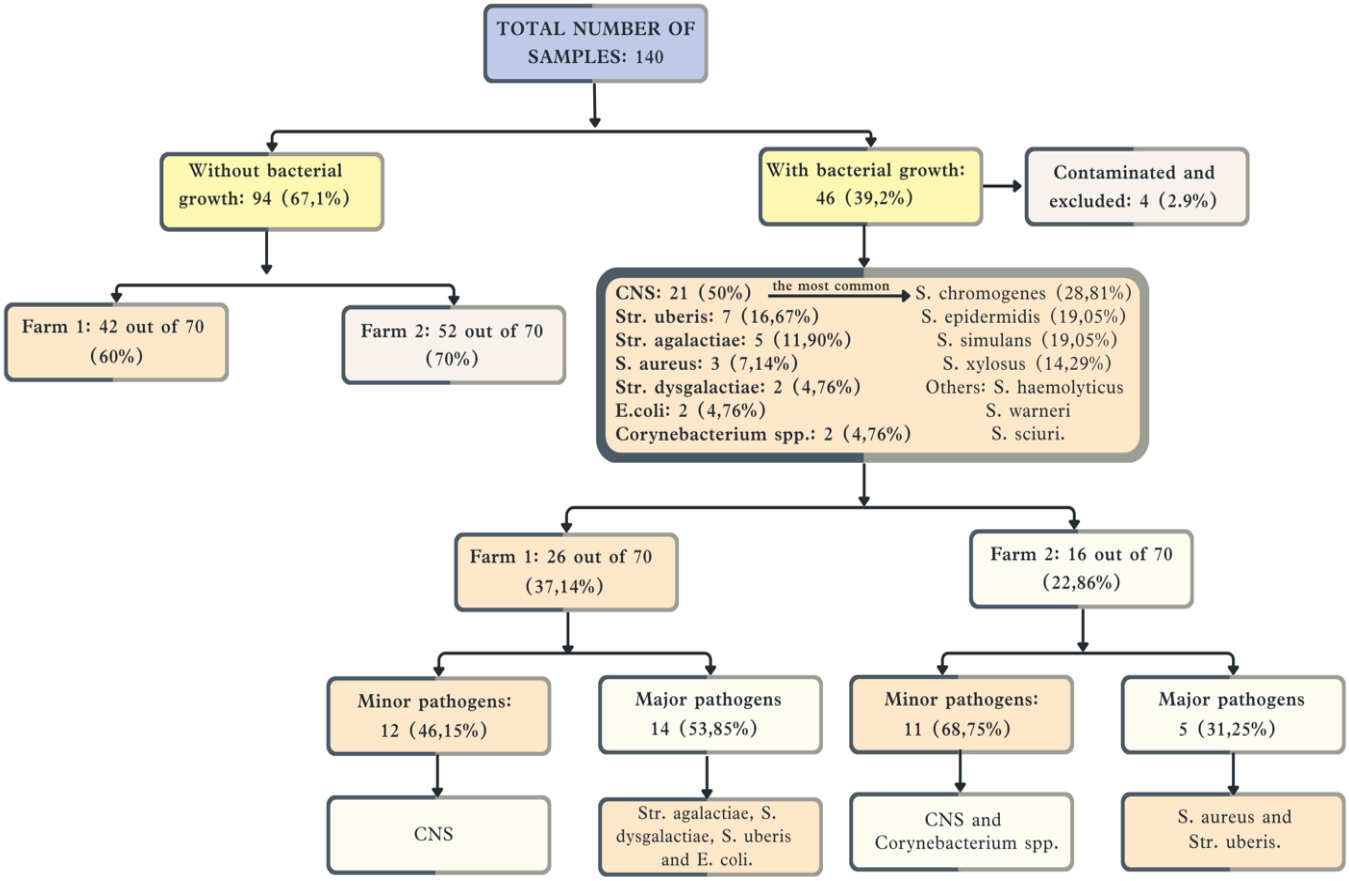

Figure 1. Prevalence of Mastitis Pathogens Identified in the Two Dairy Farms

3.2. Correlation between Bacterial Type, SCC, and DSCC

The analysis of SCC revealed significant differences between milk samples without and with bacterial infection. Samples without bacterial growth had a geometric mean SCC of 98,243 cells/mL, with a median value of 120,000 cells/mL. In samples with pathogen isolation, the mean SCC increased to 807,557 cells/mL,

with a median of 832,000 cells/mL. Notably, 23% of samples with SCC > 200,000 cells/mL showed no bacterial growth. Infections with minor pathogens were associated with a geometric mean of 423,179 cells/mL (median: 424,000), whereas infections with major pathogens exhibited much higher values (mean: 1,390,369 cells/mL; median: 1,154,000), indicating a more intense inflammatory response.

Analysis of the differential somatic cell count (DSCC) also confirmed the association with infection. Samples without bacterial growth had a mean DSCC of 26.2%, while samples with pathogens showed substantially higher values, with a mean of 68.4%. Infections with minor pathogens had a mean DSCC of 65.6%, and infections caused by major pathogens had mean values of 74.4%, highlighting the intensity of the inflammatory response according to the type of etiological agent. Considering these differences, a tentative threshold of 65% for DSCC can be suggested to indicate the presence of intramammary infection, with values above this threshold reflecting a significant inflammatory response.

At the level of specific pathogens, infections with coagulase-negative ***Staphylococcus*** *spp.* (STACN) had lower mean values (SCC – 392,520 cells/mL, median: 372,000; DSCC – 65.4%), while infections with ***Corynebacterium*** *spp.* (CORIN) were slightly higher (SCC – 815,000 cells/mL, median: 814,823; DSCC – 67.1%). Infections with ***Streptococcus*** *spp.* other than ***S. agalactiae*** (STREP), ***S. agalactiae*** (STRAG), and ***S. aureus*** (STPHA) generated intermediate mean values, with SCC ranging from 1,041,552 to 1,490,496 cells/mL and DSCC between 73.2% and 74.6%. The highest values were observed in infections with ***E. coli*** (SCC – 2,560,163 cells/mL; DSCC – 80.7%), reflecting the particularly intense inflammatory response to this pathogen. Arithmetic and geometric means, standard deviations and medians of SCC and DSCC according to bacteriological results are presented in Table 1 and Table 2.

Table 1. Variation of SCC (cells/mL) according to the presence of intramammary infection and the type of etiological agent.

SV	Category	N	AM	SD	GM	Median
Presence of infection	NO	94	129.989	92.569	98.243	120.000
	YES	42	1.066.116	769.087	807.557	832.000
Etiological agent type	Min. p	23	463.435	198.440	423.179	424.000
	Maj. p	19	1.511.737	675.311	1.390.369	1.154.000
Etiological agent	STACN	21	425.190	174.029	392.520	372.000
	STPHA	3	1.687.000	1.079.417	1.490.496	1.132.000
	STRAG	5	1.678.800	559.469	1.608.703	1.374.000
	STREP	9	1.063.111	239.626	1.041.552	972.000
	CORIN	2	815.000	24.042	814.823	815.000
	ECOLI	2	2.562.000	137.179	2.560.163	2.562.000

SV – source of variation; N – number of samples; AM – arithmetic mean; SD – standard deviation; GM – geometric mean; Min. p – minor pathogens; Maj. p – major pathogens; STACN – coagulase-negative Staphylococcus spp.; STPHA – *S. aureus*; STRAG – *S. agalactiae*; STREP – *Streptococcus* spp. other than *S. agalactiae*; CORIN – *Corynebacterium* spp.; ECOLI – *E. coli*.

Table 2. Variation of DSCC (%) according to the presence of intramammary infection and the type of etiological agent.

SV	Category	N	AM	SD	GM
Presence of infection	NO	94	26,2	19,5	30,1
	YES	42	68,4	9,7	67,9
Etiological agent type	Min. p	23	65,6	6,4	65,4
	Maj. p	19	74,4	4,6	73,4
Etiological agent	STACN	21	65,4	6,8	65,3
	STPHA	3	74,6	7,4	78
	STRAG	5	73,4	3,0	73,4
	STREP	9	73,2	3,9	71,3
	CORIN	2	67,1	1,1	67,1
	ECOLI	2	80,7	3,2	80,7

SV – source of variation; N – number of samples; AM – arithmetic mean; SD – standard deviation; Min. p – minor pathogens; Maj. p – major pathogens; STACN – coagulase-negative *Staphylococcus* spp.; STPHA – *S. aureus*; STRAG – *S. agalactiae*; STREP – *Streptococcus* spp. other than *S. agalactiae*; CORIN – *Corynebacterium* spp.; ECOLI – *E. coli*.

4. Discussion

The results obtained in our study indicate that the overall prevalence of IMI was 32.9%. The isolated bacteria were identified as *S. agalactiae*, *S. uberis*, *S. dysgalactiae*, *E. coli*, *S. aureus*, CNS, and *Corynebacterium* spp., with findings similar to those reported by other authors [14,25]. Over 80% of IMI in this study were caused by *Streptococcus spp., S. aureus*, and CNS, which contrasts with more recent studies showing a decrease in IMI caused by *S. aureus* and an increase in the prevalence of Gram-negative pathogens [26]. In Farm 1, prevalence was higher both before drying off (38.24%) and after calving (36.11%) compared to Farm 2, where values were 29.41% and 16.67%, respectively. These data suggest a possible influence of dry period management and hygiene conditions on mastitis incidence. Similar to observations reported by Haw et al. [27] and Emidio et al. [28], where "no significant growth" was the most frequent result of milk cultures (75.2% and 66.0%, respectively), in our study a considerable proportion of samples (67.1%) showed no bacterial growth. These finding highlights that many inflammatory changes in the mammary gland may be associated with non-bacterial factors or transient infections, which are difficult to detect using conventional bacteriological culture.

Regarding the distribution of etiological agents, CNS were the most frequently isolated microorganisms (50% of positive samples), followed by *S. uberis* and other major pathogens such as *S. aureus*, *S. agalactiae*, and *S. dysgalactiae*. These results are consistent with recent literature reporting non-aureus staphylococci as the most commonly identified agents involved in subclinical mastitis [27,29,30]. The predominant species in our study, *S. chromogenes*, *S. epidermidis*, and *S. simulans*, are also among the most frequently reported internationally [27,31,32]. Moreover, *S. chromogenes* and *S. simulans* have been cited in multiple studies as being associated with persistent infections and chronic subclinical mastitis [32,33], underlining the clinical relevance of their frequent isolation in the samples analyzed in our study.

Certain differences between the two farms were observed regarding pathogen distribution. In Farm 1, major pathogens predominated (53.85%), whereas in Farm 2, the largest proportion corresponded to minor pathogens (68.75%). These results suggest that environmental contamination control may be insufficient in Farm 2, while in Farm 1, cow-to-cow transmission appears to be facilitated by improper milking parlor management. Similar situations were described by Nunes De Souza et al. [14], where the distribution of infections with *S. agalactiae*, *S. aureus*, and environmental streptococci varied depending on the farm and local management practices.

Our study results highlight significant differences in SCC depending on the presence and type of pathogens. Uninfected samples showed a geometric mean of 98,243 cells/mL (median: 120,000), whereas positive samples had much higher values (mean: 807,557 cells/mL; median: 832,000), confirming the role of mammary infections in increasing SCC. SCC values in uninfected quarters generally fall within the ranges reported by Dohoo et al. [34] (113,000–251,000 cells/mL) and are comparable to Emídio et al. [28], who reported a geometric mean of 52,000 cells/mL and a median of 70,000 cells/mL, as well as the meta-analysis by Djabri et al. [35], which indicated a mean of 68,000 cells/mL, suggesting consistency and practical relevance. Regarding positive samples, the mean SCC in our study exceeds the ranges reported by Dohoo et al. [34] (190,000–519,000 cells/mL) and Nunes de Souza et al. [14] (mean 228,000 cells/mL; median 342,000), which may be explained by methodological variability, herd management, or factors related to physiological status and stress. All studies, however, confirm a clear increase in SCC in the presence of pathogens, highlighting the consistency of the mammary gland's immune response. It should be noted that in both our study and Petzer et al. [36], over 20% and 30% of samples with elevated SCC were culture-negative, emphasizing the importance of using multiple diagnostic methods for IMI.

Beyond general differences between positive and negative samples, our analysis revealed a clear separation of SCC values according to pathogen type. Infections with minor pathogens were associated with a geometric mean of 423,179 cells/mL (median: 424,000), whereas infections with major pathogens resulted in significantly higher values (mean: 1,390,369 cells/mL; median: 1,154,000), indicating a stronger inflammatory response. Previous studies [11,34] have shown that when bacteria are classified into major pathogens (streptococci, *S. aureus*, and coliforms such as *E. coli* and *Klebsiella spp*.) and minor pathogens (coryneforms and

CNS), quarters infected with major pathogens had SCC > 600,000 cells/mL on average, while minor pathogens yielded SCC between 100,000 and 300,000 cells/mL. Our results indicate even higher levels, suggesting either greater infection severity in the studied herd or differences in herd management or detection sensitivity. Similarly, Eberhart et al. [37] reported SCC increases from 190,000 to 320,000 cells/mL for minor pathogens and from 614,000 to 986,000 cells/mL for major pathogens. A relevant methodological difference between studies lies in sample type: composite milk versus milk from individual quarters. In both our study and Eberhart et al. [37], evaluations were performed on composite samples, whereas Harmon [11,34] and Dohoo et al. [34] used individual quarter samples.

Analysis of SCC by pathogen showed clear species differences: the highest geometric mean and median SCC values were recorded for *E. coli* (2,560,163 and 2,562,000 cells/mL), followed by *S. agalactiae* (1,608,703 and 1,374,000 cells/mL), *S. aureus* (1,490,496 and 1,132,000 cells/mL), and other streptococci (1,041,552 and 972,000 cells/mL). The lowest values were recorded for *Corynebacterium spp.* (815,000 and 814,823 cells/mL) and CNS (392,520 and 372,000 cells/mL). Overall, the arithmetic mean of SCC increased progressively in the order: no bacterial growth, CNS, *Corynebacterium spp*., other streptococci, *S. aureus*, *S. agalactiae*, and *E. coli.* CNS infections showed the lowest SCC, slightly above Emídio et al. [28] values (mean 138,000 cells/mL) but close to Nunes de Souza et al. [14] (mean 400,000 cells/mL; median ≤ 205,000). For *Corynebacterium* spp., the values were significantly higher compared to literature data. Nunes de Souza et al. [14] reported a mean of approximately 400,000 cells/mL (median ≤ 166,000), and Wilson et al. [25] confirmed similar values. These differences highlight the variability of the inflammatory response, likely influenced by management factors or specific characteristics of the strains involved. In the case of *Streptococcus spp.,* infections with *S. agalactiae* in our study generated a mean very close to the values reported by Djabri et al. [35] (1,572,000 cells/mL). The results are also consistent with Nunes de Souza et al. [14], who showed that *S. agalactiae* consistently produces the highest SCC values, with means of 662,000 cells/mL and medians ≥ 923,000. Wilson et al. [25] confirmed this trend, highlighting the same pathogen as responsible for the most significant increases in SCC.

For *Streptococcus spp*. other than *S. agalactiae* (e.g., *S. uberis*, *S. dysgalactiae*), our values are comparable to those reported by Emídio et al. [28], who found 1,024,000 and 547,000 cells/mL, respectively, but higher than those mentioned by Nunes de Souza et al. [14], where means were around 800,000 cells/mL, with medians ≥ 641,000. Regarding *S. aureus*, the SCC values observed in our study significantly exceed the means reported by Emídio et al. [28] (357,000 cells/mL) and Djabri et al. [35] (587,000 cells/mL) but are close to those in the study by Nunes de Souza et al. [14] (966,000 cells/mL, median ≥ 509,000). This variation between studies may be partly explained by the intermittent shedding of the bacterium in milk, a characteristic of *S. aureus*, which influences SCC levels [38] and can lead to differences in reported means. The results also confirm *S. aureus* as one of the pathogens most frequently associated with high SCC values. The highest values in our study were associated with *E. coli* (2,560,163 cells/mL), confirming the intensity of the inflammatory response to Gram-negative pathogens. Djabri et al. [35] and Harmon [11] also reported that *E. coli* causes the highest SCC levels, typically in the context of clinical mastitis, which aligns with our observations. Overall, comparison of our results with the literature reveals the same general trends: CNS and *Corynebacterium* spp. result in low to moderate SCC values, *S. aureus* and streptococci are associated with intermediate to high values, and Gram-negative pathogens, especially *E. coli*, induce the highest SCC levels.

Additionally, the DSCC analysis conducted in our study confirmed its correlation with the presence of IMI. Samples with no bacterial growth recorded a mean DSCC of 26.2%, while positive samples showed significantly higher values, with a mean of 68.4%. Infections caused by minor pathogens were associated with a mean DSCC of 65.6%, whereas those caused by major pathogens showed a mean of 74.4%, highlighting the differentiated intensity of the inflammatory response depending on the type of etiological agent. To the best of our knowledge, the dynamics of DSCC in relation to pathogen type are very poorly described in the literature, which limits the interpretation of results at a longitudinal level. Nevertheless, our findings are consistent with the observations of Schwarz et al. [20], who reported that most cases of IMI caused by major pathogens showed high DSCC values (>60%). In contrast, in IMI caused by minor pathogens, DSCC varied considerably (14–89%), a variation attributed mainly to the different levels of pathogenicity of NAS [39]. The significantly higher DSCC values in cows with IMI caused by major pathogens can be explained by the fact that this parameter primarily reflects the proportion of PMN [15], immune cells known to be dominant in the presence of major pathogens [16]. Conversely, Kirkeby et al. [21] demonstrated that DSCC appears to be a useful indicator for the presence of any pathogen, but less specific for differentiating between pathogen groups.

Based on the differences observed in this study, our results suggest a preliminary threshold of 65% for DSCC, with values above this level indicating a significant inflammatory response and, consequently, the presence of intramammary infection. This threshold aligns with values proposed in the scientific literature, where DSCC between 65% and 72% has been suggested as an indicative cut-off for the detection of subclinical mastitis [15]. Furthermore, Schwarz et al. [20] reported that at an SCC of 200,000 cells/mL, a DSCC > 60% may signal mammary gland infection (sensitivity 67–87%), while Zecconi et al. [40] identified DSCC thresholds differentiated by days in milk (66.3% for <100 DIM, 69.2% for 101–200 DIM, and 69.3% for >200 DIM), with an accuracy of 81% and sensitivity of 67%. Our tentative threshold of 65% falls within the range proposed by these studies, confirming overall agreement while also emphasizing the need to adjust reference values according to the specific context of each herd and local management conditions. Recent studies highlight that DSCC, in combination with SCC, can identify more IMI cases compared to SCC alone, suggesting its high potential for widespread use in udder health monitoring [20,40,41]. This approach can be particularly useful in selective dry cow therapy (SDCT), for the accurate identification of animals requiring treatment. It should be noted that, given the relatively small number of samples analyzed in our study, the 65% threshold cannot be considered definitive and applies strictly within the context of this research. In practice, DSCC values should be interpreted alongside other clinical and laboratory criteria to accurately assess the health status of dairy cows.

The main limitation of this study is the relatively small number of samples and farms included, which may affect the generalizability of the results. Additionally, sampling was conducted at relatively infrequent intervals, which may not fully capture the rapid dynamics of DSCC and SCC changes during the course of infection. The lack of detailed differentiation by lactation stage and parity represents another limitation, given the known impact of these factors on the inflammatory response. For future research, studies involving larger herds and more frequent sampling are needed to better capture the variability and progression of DSCC over time. Integrating DSCC with other parameters (SCC, milk yield, lactation stage) into complex predictive models could improve the diagnosis and management of mastitis**.** Furthermore, validating DSCC thresholds according to each farm's context and the characteristics of the pathogens involved will be essential for practical applicability.

5. Conclusions

The main bacteria identified in this study included both major pathogens (*E. coli*, *S. agalactiae*, *S. uberis*, *S. dysgalactiae*, and *S. aureus*) and minor pathogens (CNS, *Corynebacterium* spp.), each exerting a different influence on the inflammatory response (as reflected by SCC and DSCC) and milk quality. Their distribution varied between farms, with higher prevalence observed on Farm 1, both before dry-off and after calving. This highlights the importance of proper dry period management and minimizing cow-to-cow transmission, along with careful monitoring of udder health through SCC and DSCC, key tools for the prevention and control of mastitis.

Author Contributions: Conceptualization, L.M.B and I.D.U.; methodology, I.D.U.; software, I.D.U.; S.C (Ștefan Coman); validation, L.M.B. D.I.B. and S.C (Simona Ciupe); formal analysis, I.D.U.; investigation, I.D.U.; data curation, I.D.U.; writing—original draft preparation, I.D.U; writing—review and editing, D.I.B.; visualization, S.C; supervision, L.M.B.; project administration, L.M.B.; funding acquisition, L.M.B. All authors have read and agreed to the published version of the manuscript".

Funding: This research received no external funding.

Institutional Review Board Statement: The study was approved by the Ethics Committee of the University of Agricultural Sciences and Veterinary Medicine, Cluj-Napoca (514/10.04.2025).

Conflicts of Interest: The authors declare no conflict of interest.

References

1. Tommasoni, C.; Fiore, E.; Lisuzzo, A.; Gianesella, M. Mastitis in Dairy Cattle: On-Farm Diagnostics and Future Perspectives. *Animals* **2023**, *13*, 2538.
2. Williamson, J.; Callaway, T.; Rollin, E.; Ryman, V. Association of Milk Somatic Cell Count with Bacteriological Cure of Intramammary Infection—A Review. *Agriculture* (Switzerland) **2022**, *12*.
3. N. Sharma, N.K.S. and M.S.B. Relationship of Somatic Cell Count and Mastitis: An Overview. *Asian-Aust J Anim Sci* **2011**, *24*, 429–438.

4. Abdi, R.D.; Gillespie, B.E.; Ivey, S.; Pighetti, G.M.; Almeida, R.A.; Dego, O.K. Antimicrobial Resistance of Major Bacterial Pathogens from Dairy Cows with High Somatic Cell Count and Clinical Mastitis. *Animals* **2021**, *11*, 1–14, doi:10.3390/ani11010131.
5. Batavani, R.A.; Asri, S.; Naebzadeh, H. The Effect of Subclinical Mastitis on Milk Composition in Dairy Cows. *Iran J Vet Res* **2007**, *8(3)*, 227.
6. Koess, C.; Hamann, J. Detection of Mastitis in the Bovine Mammary Gland by Flow Cytometry at Early Stages. *J Dairy Res* **2008**, *75*, 225–232, doi:10.1017/S0022029908003245.
7. Sumon, S.M.M.R.; Parvin, M.S.; Ehsan, M.A.; Islam, M.T. Dynamics of Somatic Cell Count and Intramammary Infection in Lactating Dairy Cows. *J Adv Vet Anim Res* **2020**, *7*, 314–319, doi:10.5455/JAVAR.2020.G423.
8. Green, M.J.; Green, L.E.; Schukken, Y.H.; Bradley, A.J.; Peeler, E.J.; Barkema, H.W.; De Haas, Y.; Collis, V.J.; Medley, G.F. Somatic Cell Count Distributions during Lactation Predict Clinical Mastitis. *J Dairy Sci* **2004**, *87*, 1256–1264, doi:10.3168/jds.S0022-0302(04)73276-2.
9. Kandeel, S.A.; Megahed, A.A.; Arnaout, F.K.; Constable, P.D. Evaluation and Comparison of 2 On-Farm Tests for Estimating Somatic Cell Count in Quarter Milk Samples from Lactating Dairy Cattle. *J Vet Intern Med* **2018**, *32*, 506–515, doi:10.1111/jvim.14888.
10. Valldecabres, A.; Clabby, C.; Dillon, P.; Silva, P.; Graphical, B. Association between Quarter-Level Milk Somatic Cell Count and Intramammary Bacterial Infection in Late-Lactation Irish Grazing Dairy Cows; *JDS communications*, **2023,** *4(4)*, 274-277.
11. Harmon, R.J. Physiology of Mastitis and Factors Affecting Somatic Cell Counts. *J Dairy Sci* **1994**, *77*, 2103–2112, doi:10.3168/jds.S0022-0302(94)77153-8.
12. Condas, L.A.Z.; De Buck, J.; Nobrega, D.B.; Carson, D.A.; Roy, J.P.; Keefe, G.P.; DeVries, T.J.; Middleton, J.R.; Dufour, S.; Barkema, H.W. Distribution of Non-Aureus Staphylococci Species in Udder Quarters with Low and High Somatic Cell Count, and Clinical Mastitis. *J Dairy Sci* **2017**, *100*, 5613–5627, doi:10.3168/jds.2016-12479.
13. Taponen, S.; Liski, E.; Heikkilä, A.M.; Pyörälä, S. Factors Associated with Intramammary Infection in Dairy Cows Caused by Coagulase-Negative Staphylococci, Staphylococcus Aureus, Streptococcus Uberis, Streptococcus Dysgalactiae, Corynebacterium Bovis, or Escherichia Coli. *J Dairy Sci* **2017**, *100*, 493–503, doi:10.3168/jds.2016-11465.
14. Nunes De Souza, G.; Vasconcelos, M.A.; Brito, P.; Vinícius, M.; Barbosa Da Silva, G. Somatic Cell Counts Variation in Dairy Cows According to Mastitis Pathogens; *Arq Bras Med Vet Zootec*, **2009**, *61*, 1015-1020;
15. Damm, M.; Holm, C.; Blaabjerg, M.; Bro, M.N.; Schwarz, D. Differential Somatic Cell Count—A Novel Method for Routine Mastitis Screening in the Frame of Dairy Herd Improvement Testing Programs. *J Dairy Sci* **2017**, 100, 4926–4940, doi:10.3168/jds.2016-12409.
16. Paape, M.J.; Wergin, W.P.; Guidry, A.J.; Pearson, R.E. Leukocytes–Second Line of Defense Against Invading Mastitis Pathogens. *J Dairy Sci* **1979**, *62*, 135–153, doi:10.3168/jds.S0022-0302(79)83215-4.
17. Dal Prà, A.; Biscarini, F.; Cavani, G.L.; Bacchelli, S.; Iotti, A.; Borghi, S.; Nocetti, M.; Moroni, P. Relationship between Total and Differential Quarter Somatic Cell Counts at Dry-off and Early Lactation. *PLoS One* **2022**, *17*, doi:10.1371/journal.pone e0275755.
18. Kirkeby, C.; Toft, N.; Schwarz, D.; Farre, M.; Nielsen, S.S.; Zervens, L.; Hechinger, S.; Halasa, T. Differential Somatic Cell Count as an Additional Indicator for Intramammary Infections in Dairy Cows. *J Dairy Sci* **2020**, *103*, 1759–1775, doi:10.3168/jds.2019-16523.
19. Pegolo, S.; Tessari, R.; Bisutti, V.; Vanzin, A.; Giannuzzi, D.; Gianesella, M.; Lisuzzo, A.; Fiore, E.; Barberio, A.; Schiavon, E.; et al. Quarter-Level Analyses of the Associations among Subclinical Intramammary Infection and Milk Quality, Udder Health, and Cheesemaking Traits in Holstein Cows. *J Dairy Sci* **2022**, *105*, 3490–3507, doi:10.3168/jds.2021-21267.
20. Schwarz, D.; Santschi, D.E.; Durocher, J.; Lefebvre, D.M. Evaluation of the New Differential Somatic Cell Count Parameter as a Rapid and Inexpensive Supplementary Tool for Udder Health Management through Regular Milk Recording. *Prev Vet Med* **2020**, *181*, doi:10.1016/j.prevetmed.2020.105079.
21. Kirkeby, C.; Schwarz, D.; Denwood, M.; Farre, M.; Nielsen, S.S.; Gussmann, M.; Toft, N.; Halasa, T. Dynamics of Somatic Cell Count (SCC) and Differential SCC during and Following Intramammary Infections. *J Dairy Sci* **2021**, *104*, 3427–3438, doi:10.3168/jds.2020-19378.
22. Schwarz, D.; Kleinhans, S.; Reimann, G.; Stückler, P.; Reith, F.; Ilves, K.; Pedastsaar, K.; Yan, L.; Zhang, Z.; Lorenzana, R. Associations between Different Udder Health Groups Defined Based on a Combination of Total and Differential Somatic Cell Count and the Future Udder Health Status of Dairy Cows. *Prev Vet Med* **2021**, *192*, doi:10Plea.1016/j.prevetmed.2021105374.
23. Adkins, P.R.F., Middleton, J.R., Fox, I.K., Pighetti, G., Petersson-Wolfe, C., **2017**. Laboratory Handbook on Bovine Mastitis. National Mastitis Council, New Prague, MN, USA, 2017.
24. Harmon, R.J.; Eberhart, R.J.; Jasper, D.E.; Langlois, B.E.; Wilson, R.A. Microbiological Procedures for the Diagnosis of Bovine Udder Infection. Arlington: National Mastitis Council **1990**, p. 34.
25. Wilson, D.J.; Gonzalez, R.N.; Das, H.H. Bovine Mastitis Pathogens in New York and Pennsylvania: Prevalence and Effects on Somatic Cell Count and Milk Production. *J Dairy Sci* **1997**, *80*, 2592–2598, doi:10.3168/jds.s0022-0302(97)76215-5.
26. Ruegg, P.L. A 100-Year Review: Mastitis Detection, Management, and Prevention. *J Dairy Sci* **2017**, 100, 10381–10397, doi:10.3168/jds.2017-13023.

27. Haw, S.R.; Adkins, P.R.F.; Bernier Gosselin, V.; Poock, S.E.; Middleton, J.R. Intramammary Infections in Lactating Jersey Cows: Prevalence of Microbial Organisms and Association with Milk Somatic Cell Count and Persistence of Infection. *J Dairy Sci* **2024**, 107, 3157–3167, doi:10.3168/jds.2023-23848.
28. Emídio, J.; Lopes, F.; Carla, J.I.; Ii, C.L.; Aparecida, M.; Paiva, V.; Ii, B.; Ribeiro, F.; Iii, S.; Aurélio, M.; et al. Relationship between Total Bacteria Counts and Somatic Cell Counts from Mammary Quarters Infected by Mastitis Pathogens, *Ciência Rural*, Santa Maria, **2012**, *42(4)*, 691-696, ISSN 0103-8478.
29. Zigo, F.; Farkasová, Z.; Vyrostková, J.; Regecová, I.; Ondrasovicová, S.; Vargová, M.; Sasáková, N.; Pecka-Kielb, E.; Bursová, S.; Kiss, D.S. Dairy Cows' Udder Pathogens and Occurrence of Virulence Factors in Staphylococci. *Animals* **2022**, *12(4)*, 470, doi:10.3390/ani12040470.
30. Heikkilä, A.M.; Liski, E.; Pyörälä, S.; Taponen, S. Pathogen-Specific Production Losses in Bovine Mastitis. *J Dairy Sci* **2018**, 101, 9493–9504, doi:10.3168/jds.2018-14824.
31. Taponen, S.; Myllys, V.; Pyörälä, S. Somatic Cell Count in Bovine Quarter Milk Samples Culture Positive for Various Staphylococcus Species. *Acta Vet Scand* **2022**, *64*, 32, doi:10.1186/s13028-022-00649-8.
32. Fry, P.R.; Middleton, J.R.; Dufour, S.; Perry, J.; Scholl, D.; Dohoo, I. Association of Coagulase-Negative Staphylococcal Species, Mammary Quarter Milk Somatic Cell Count, and Persistence of Intramammary Infection in Dairy Cattle. *J Dairy Sci* **2014**, *97*, 4876–4885, doi:10.3168/jds.2013-7657.
33. Valckenier, D.; Piepers, S.; De Visscher, A.; De Vliegher, S. The Effect of Intramammary Infection in Early Lactation with Non-Aureus Staphylococci in General and Staphylococcus Chromogenes Specifically on Quarter Milk Somatic Cell Count and Quarter Milk Yield. *J Dairy Sci* **2020**, *103*, 768–782, doi:10.3168/jds.2019-16818.
34. Dohoo, I.R.; Meek, A.H. Somatic Cell Counts in Bovine Milk, *Can Vet J* **1982**, 23.4: 119.
35. Djabri, B.; Bareille, N.; Beaudeau, F.; Seegers, H. Quarter Milk Somatic Cell Count in Infected Dairy Cows: A Meta-Analysis. *Vet Res* **2002**, *33*, 335–357, doi:10.1051/vetres:2002021.
36. Petzer, I.M.; Karzis, J.; Donkin, E.F.; Webb, E.C.; Etter, E.M.C. Validity of Somatic Cell Count as Indicator of Pathogen-Specific Intramammary Infections. *J S Afr Vet Assoc* **2017**, 88, 1-10, doi:10.4102/jsava.v88i0.1465.
37. Eberhart, R.J.; Hutcidnson, L.J.; Spencer, S.B. Relationships of Bulk Tank Somatic Cell Counts to Prevalence of Intramammary Infection and to Indices of Herd Production 1; **1982**, *45*, 1125-1128.
38. Mues, L.; Kemper, N.; Blumenberg, J.A. Occurrence and Diagnostic of Intermittent Shedding of Staphylococcus Aureus in Bovine Mammary Infection. *Front Vet Sci* **2025**, *12*, 1523698.
39. Vanderhaeghen, W.; Piepers, S.; Leroy, F.; Van Coillie, E.; Haesebrouck, F.; De Vliegher, S. Identification, Typing, Ecology and Epidemiology of Coagulase Negative Staphylococci Associated with Ruminants. *Vet J*, **2015**, *203*, 44–51.
40. Zecconi, A.; Dell'orco, F.; Vairani, D.; Rizzi, N.; Cipolla, M.; Zanini, L. Differential Somatic Cell Count as a Marker for Changes of Milk Composition in Cows with Very Low Somatic Cell Count. *Animals* **2020**, *10(4)*, 604, doi:10.3390/ani10040604.
41. Schwarz, D.; Lipkens, Z.; Piepers, S.; De Vliegher, S. Investigation of Differential Somatic Cell Count as a Potential New Supplementary Indicator to Somatic Cell Count for Identification of Intramammary Infection in Dairy Cows at the End of the Lactation Period. *Prev Vet Med* **2019**, *172*, 104803 doi:10.1016/j.prevetmed.2019.104803.

CVJ CLUJ VETERINARY JOURNAL

Research Article

Histological Evaluation of Peri-Implant Soft Tissue Response to Direct Contact with Titanium Screw Surface in a Rabbit Model

Bianca Fernea [1], Aurel Damian [1], Florin Gheorghe Stan [1], Cosmin-Rareș Creț [2], Dalma Pivariu [1], Melania Ioana Crișan [1], Irina Irimescu [3]*

[1] University of Agricultural Sciences and Veterinary Medicine, Faculty of Veterinary Medicine, 3–5 Manastur Street, Cluj-Napoca, 400372, Cluj, Romania;
[2] SC Cosmin Cowvet SRL, 296/B Main Street, Inau, Salaj, Romania
[3] Long Island University, 720 Northern Blvd., Brookville, NY 11548, USA
* Correspondence: melania.crisan@usamvcluj.ro

Abstract: Rabbits present biological features that make them suitable for morphological and histological investigations that allow a closer approximation to human tissue responses, particularly with respect to immune and vascular reactions. Titanium screws measuring 5 mm in length and 2 mm in diameter were inserted into the femoral bone of five 14-month-old female rabbits of a common breed, one on the right side and one on the left. Femoral segments containing the implants were subsequently harvested, fixed in 10% formalin, decalcified with trichloroacetic acid, and embedded in paraffin. Sections 5 μm thick were cut, stained using the Goldner trichrome method, and microscopically examined. At the interface between the surface of the screw head and the newly formed tissues, a separating capsule was formed through condensation of the connective tissue. Within the medullary cavity, the bone marrow that encountered the screw surface responded by gradually regenerating with tissue of the same type, and did not exhibit a significant foreign body reaction, demonstrating a remarkable tolerance toward titanium implants. This tolerance allowed peri-implant tissues to undergo repair through the formation of tissues like those present prior to surgery. The distance between the implant surface and the surrounding tissue elements did not represent a critical factor, whereas repetitive tissue movements triggered a protective response manifested by the formation of a separating capsule between the surface of the implant head and the adjacent structures.

Keywords: rabbit, experimental, implants.

Received: 28.01.2026
Accepted: 30.01.2026
Published: 27.02.2026

DOI:10.52331/V31i16t27

1. Introduction

Rabbits present biological features that make them suitable for morphological and histological investigations. The insertion of titanium implants into cortical bone in female rabbits is accompanied by injury to all tissues in the intervention area. These tissues include the bone in which the drilling site is created, as well as the supraperiosteal soft tissues and those within the medullary cavity, namely the bone marrow. After closure of the surgical wound, the implant surface is in direct contact with all these tissues. The process of implant osseointegration within bone closely resembles the one of fracture healing. For fractures to heal under normal conditions, the fractured ends must be stabilized in such a way that the distance between them is as small as possible. It is also necessary that there is no movement beyond a certain limit between the bone ends, as excessive motion may lead to the formation of a nonunion – pseudarthrosis [1]. This situation also applies to implants, where neither the gap nor the micromotion between components should exceed 150 μm; otherwise, there is a risk of connective tissue proliferation instead of bone formation [2].

These considerations apply to the relationship between the surface of the titanium implant and the surface of the insertion site wall, where the distances can be controlled by the surgical procedure used for implant placement. The situation is different in the case of contact between implant regions that do not come into direct contact with the bone

wall but instead interface with soft tissues. In this case, the only fixed surface is that of the implant, whereas the soft tissues lack a stable shape, and their structural elements may be located at small, large, or even very large distances from the implant surface. This raises the question of whether these distances influence reparative processes in such a way that, around the implant head and the portion that penetrates the endosteum and enters the bone marrow, connective scar tissue is formed.

The aim of the study was to evaluate the tissues proliferating in the immediate vicinity of the screw head, which encounters supraperiosteal soft tissues, and of the implant portion that penetrates the bone marrow.

2. Materials and Methods

This study was conducted in strict accordance with the recommendations of the National Institutes of Health's Guide for the Care and Use of Laboratory Animals. The research protocol with animal experimentation was approved by the Scientific Ethics Committee of University of Agricultural Sciences and Veterinary Medicine (Protocol Number: 219 of 10.07.2020). All surgery was performed under anesthesia, and every effort was made to minimize suffering. Anesthesia was achieved by intramuscular administration of xylazine (5 mg/kg) and ketamine (40 mg/kg).

Titanium screws measuring 5 mm in length and 2 mm in diameter were inserted into the femoral bone of five 14-month-old female rabbits of a common breed, one on the right side and one on the left. Preparation of the surgical site consisted of clipping and disinfection with iodine tincture. followed by an incision of the skin and underlying tissues to expose the femur. The insertion site was drilled using a 1.8-mm diameter drill bit, with continuous cooling of the area using physiological saline. The screws were inserted in such a manner that they penetrated the endosteum and entered the medullary cavity to an appreciable extent. After routine closure of the surgical wound, Enroxil 5% (enrofloxacin) was administered subcutaneously at a dose of 20 mg/kg for 5 days as antimicrobial prophylaxis, and Meloxicam was given as an analgesic at a dose of 1 mg/kg subcutaneously for 3 days. In this experimental study, death constituted the predefined experimental endpoint. Animals were monitored daily throughout the study period for general health status, behavior, food and water intake, locomotion, and surgical site condition. No animals reached criteria requiring premature euthanasia. At the end of the two-month experimental period, all animals were humanely euthanized by a veterinarian by using a method in accordance with the provisions of EU Directive 2010/63/EU on the protection of animals used for scientific purposes (administration of an overdose of sodium phenobarbital). Death was confirmed prior to tissue collection by the absence of heartbeat/respiration and corneal reflex.

Femoral segments containing the implants were subsequently harvested, fixed in 10% formalin, decalcified with trichloroacetic acid, and embedded in paraffin. Sections 5 μm thick were cut, stained using the Goldner trichrome method, and examined under an Olympus BX41 microscope.

3. Results

Histological processing allowed the preparation of sections encompassing the entire surgical area, enabling assessment of all components in contact with the implant, including both hard osseous tissues and soft tissues located supraperiosteally as well as those within the medullary canal (Fig. 1a).

It was observed that the supraperiosteal area was repaired by newly proliferated tissues, consisting of loose connective tissue in which muscle fiber bundles were evident. At the interface between the surface of the screw head and the newly formed tissues, a separating capsule was formed through condensation of the connective tissue (Fig. 1b). Within the medullary cavity, the bone marrow that met the screw surface did not exhibit a significant reaction, in the sense that there was no tendency toward connective tissue proliferation. This demonstrates that the presence of the titanium implant was well tolerated by the bone marrow (Fig. 1c).

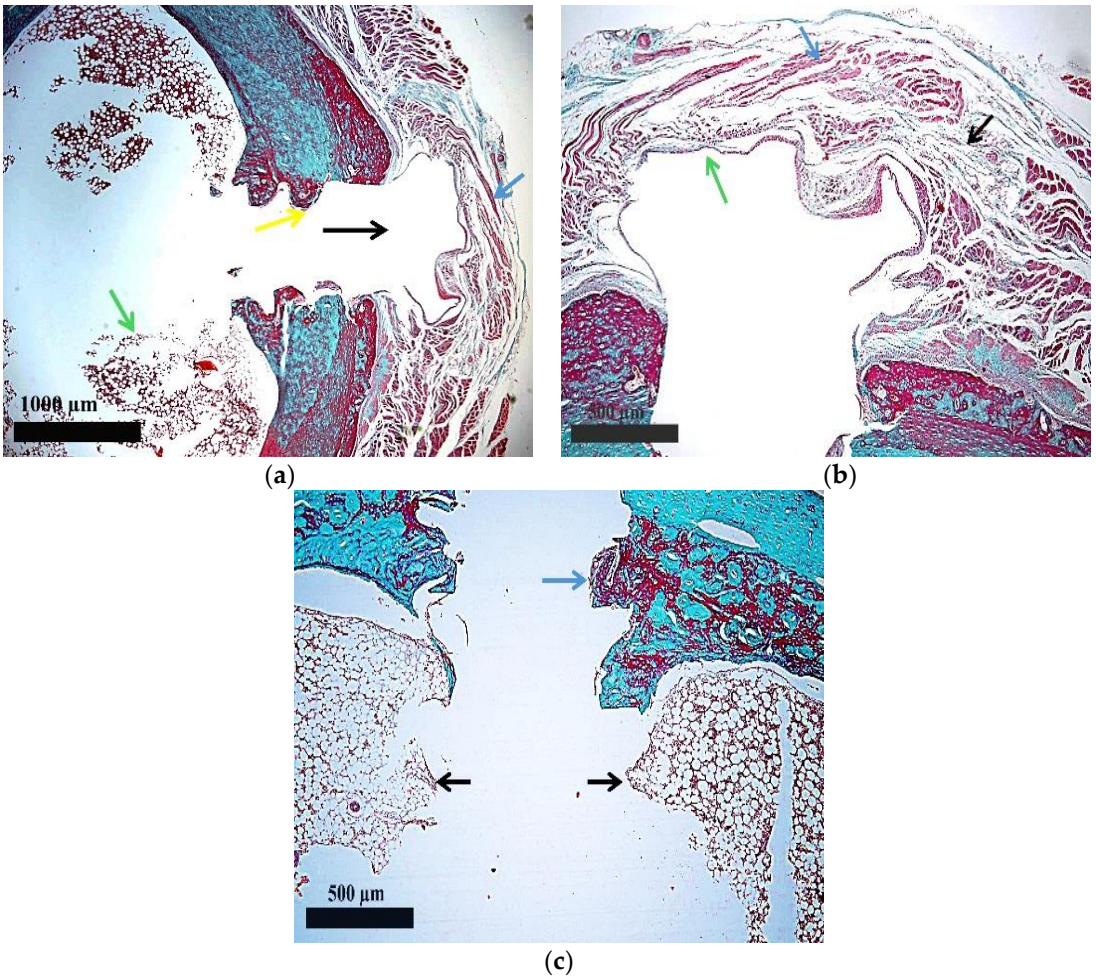

(**a**) (**b**)

(**c**)

Figure 1. (**a**) Surgical site: black arrow—implant location; blue arrow—supraperiosteal soft tissues; green arrow—bone marrow; yellow arrow—bone–implant interface (Goldner trichrome, 2× objective); (**b**) Supraperiosteal soft tissues: black arrow—loose connective tissue; blue arrow—muscle tissue; green arrow—connective tissue capsule (Goldner trichrome, 4x objective); (**c**) Intramedullary soft tissues: black arrow—bone marrow; blue arrow—bone–implant interface (Goldner trichrome, 4× objective).

4. Discussion

The proliferation of reparative tissues following the insertion of a titanium implant is a complex process that differs in duration depending on the type of tissue involved. The repair of bone tissue at the bone–implant interface takes the longest, whereas peri-implant soft tissues regenerate over a significantly shorter period. Most available information concerns the evolution of reparative processes at the bone–implant interface, as this region ensures secondary stability of the implants and their long-term persistence in the body. It is known that the distance between the implant surface and the bony wall of the insertion site should not exceed a certain limit, since at greater distances connective tissue will proliferate instead of the desired bone tissue [2]. Along this portion of the interface, the distances between components can be planned and achieved through the surgical technique employed, so that from this perspective the conditions are under control. Such control cannot be exerted at the interface between the implant surface and soft tissues, because in this case only the implant surface is fixed and rigid. In relation to it, the components of the soft tissues are located at varying distances, and some of them may undergo displacement within certain limits, either relative to each other or to the implant surface. This mainly refers to the soft tissues covering the surface of the implant head. Repair of these tissues occurred in a natural manner, with loose connective tissue containing bundles of muscle fibers.

It should be noted that this loose connective tissue showed no tendency toward fibrous consolidation, which demonstrates that tissue repair in this area was not negatively influenced by the presence of the titanium implant. From this perspective, it can be stated that the peri-implant soft tissues organism tolerated

the titanium implant very well. The current results are consistent with other experiments conducted on rabbits [3-11].

However, a separating connective tissue capsule was formed between the surface of the screw head and the tissues covering it. It can be considered that this capsule did not develop as a reaction of the organism to the material from which the implant was made, nor because of the distance between the surface of the implant head and the components of the adjacent loose connective tissue. Rather, its appearance seemed to be a consequence of the fact that the tissue covering the implant head undergoes movement due to contraction of the neighboring muscle tissue. These movements generated a certain degree of friction between the components of the connective tissue and the hard surface of the implant, and the organism responded by organizing this separating capsule between the loose tissue and the implant surface. By covering the implant head, this capsule protected the loose connective tissue so that it did not experience direct contact with the hard implant surface during the relatively frequent movements to which it was subjected.

Within the medullary cavity, the situation was also particular, in that the bone marrow showed no signs of injury nor proliferation of undesirable tissues, such as connective tissue. In other words, although the marrow was traumatized to a certain depth during the procedure required for implant insertion, it responded by gradually regenerating with tissue of the same type, namely bone marrow. This demonstrates that the marrow did not react to the presence of the implant as to a foreign body; on the contrary, it exhibited a remarkable tolerance toward it. Moreover, the distance between the implant surface and the components of the marrow was greater than that between the implant surface and the bony wall, and even greater than that between the implant surface and the constituent elements of the connective tissue covering the implant head. Nevertheless, this distance did not constitute a major problem capable of inducing the formation of separating structures, as observed in the case of the supraperiosteal tissues covering the screw head. It can therefore be stated that the distance between components did not significantly influence reparative processes in the case of all tissues adjacent to the surface of titanium screws.

When the peri-implant soft tissues were comparatively evaluated in terms of their response to proximity with the surface of titanium screws, it was evident that they tolerated this relationship very well. In this context, the injured tissues were repaired by the same tissue types that had been present in the area prior to the surgical intervention. Nevertheless, a separating capsule developed between the implant head and the newly proliferated tissues, whereas no such structure was observed between the bone marrow and the implant.

This formation did not appear to represent a rejection response to the implant material, nor was it related to the distance between the screw surface and the surrounding tissue elements. Instead, it appeared to have an objective cause specific to the anatomical region involved. A distinctive feature of the tissues covering the implant head was their composition, consisting of loose connective tissue containing bundles of muscle fibers. Through contraction of these muscles, the structural elements of the loose connective tissue underwent displacement within certain limits. Consequently, these tissues exhibited repetitive mobility, which subjected those in direct contact with the implant surface to friction against the rigid surface of the implant. This friction was perceived as a repetitive mechanical aggression, leading to the organization of a protective separating capsule that eliminated direct friction between the adjacent tissues and the implant surface.

5. Conclusions

Most of the studies focus on osseointegration and hard tissue responses to titanium implants. This research emphasizes the biological behavior of soft tissues at the implant interface, offering detailed microscopic evidence of tissue organization. In conclusion, supraperiosteal and medullary soft tissues exhibited a high degree of tolerance toward titanium implants, without evidence of foreign body reactions. This tolerance allowed peri-implant tissues to undergo repair through the formation of tissues like those present prior to surgery. The distance between the implant surface and the surrounding tissue elements did not represent a critical factor, whereas repetitive tissue movements triggered a protective response manifested by the formation of a separating capsule between the surface of the implant head and the adjacent structures. The current study is relevant for implant dentistry and biomaterials, as it supports the optimization of implant surface design and surgical protocols aimed at improving long-term clinical outcomes and reducing peri-implant complications.

Author Contributions:

Conceptualization: A.D., M.I.C.; Methodology: B.F., A.D., F.G.S.; Investigation: B.F., D.P., C.-R.C.; Histological analysis: B.F., I.I.; Writing – original draft: B.F., M.I.C.; Writing – review and editing: M.I.C., I.I.; Supervision: A.D., M.I.C. All authors have read and agreed to the published version of the manuscript.

Funding: This research received no external funding.

Institutional Review Board Statement: The study was conducted according to the guidelines of the Declaration of Helsinki, and approved by the Ethics Committee of the University of Agricultural Sciences and Veterinary Medicine (Protocol Number: 219 of 10.07.2020).

Conflicts of Interest: The authors declare no conflict of interest.

References

1. Kuzyk, P.R.T.; Schemitsch, E.H. The basic science of peri-implant bone healing. *Indian J Orthop* **2011**, *45*(2), 108–115. DOI: 10.4103/0019-5413.77129
2. Pilliar, R.M.; Lee, J.M.; Maniatopoulos, C. Observations on the effect of movement on bone ingrowth into porous-surfaced implants. *Clin Orthop Relat Res* **1986**, *208*, 108–113. PMID: 3720113.
3. Marcu, T.; Gal, A.F.; Rațiu, C.A.; Damian, A.; Rațiu, I.A. Adaptive structures proliferated in the rabbit shoulder eight weeks after titanium implant insertion. *J Osseointegration Oral Rehabil* **2022**, *14*(3), 180–184. DOI 10.23805/JO.2022.14.24
4. Pantor, M.; Rațiu, C.A.; Ciavoi, G.; Rațiu, I.A.; Maghiar, L.; Maghiar, A.M. Hematogenous marrow tolerance in direct contact with a titanium implant. *Acta Stomatol Marisiensis* **2022**, *5*(2), 43–50. DOI: 10.2478/asmj-2022-0011
5. Rațiu, C.A.; Rațiu, I.A.; Miclăuș, V.; Pantor, M.; Rus, V.; Martonoș, C.O.; Lacatus, R.; Purdoiu, R.C.; Gal, A.F. The influence of haematogenous bone marrow on early osseointegration of a titanium implant penetrating the endosteum. *Int J Morphol* **2022**, *40*(1), 188–193. DOI:10.4067/S0717-95022022000100188
6. Rațiu, C.A.; Sinescu, C.; Dejeu, D.; Tica, O.; Moisa, C.; Croitoru, C.A.; Rațiu, I.A.; Duma, V.F.; Todor, A.; Miclăuș, V.; Rus, V. Participation of the periosteum, endosteum, and hematogenous marrow in early osseointegration of a titanium implant inserted in contact with hematogenous marrow. *Medicina* **2025**, *61*, 1841. DOI: 10.3390/medicina61101841
7. Sabou, I.; Gal, A.F.; Matei-Lațiu, M.C.; Rus, V.; Miclăuș, V.; Rațiu, C.; Martonos, C.O.; Oros, N.; Oana, L. Does the diameter of the titanium orthopaedic screw insertion hollow influence the mechanism of contact osteogenesis? A comparative assessment in female rabbit femoral bone. *Rev Rom Med Vet* **2023**, *33*(4), 27–32. ISSN: 1220-3173; E-ISSN: 2457-7618 WOS:001165288300002
8. Sabou, I.; Gherman (Dragomir), M.F.; Ober, C.; Miclăuș, V.; Rațiu, C.; Oros, N.; Alexandru, B.C.; Oana, L. Consolidation structures proliferated around a titanium implant inserted into the female rabbit femur through an orifice smaller than the screw core. *Int J Morphol* **2025**, *43*(2), 600–605. DOI:10.4067/S0717-95022025000200600
9. Duma, V.; Gal, A.F.; Rus, V.; Matei-Lațiu, M.C.; Rațiu, C.; Alexandru, B.C.; Lațiu, C.; Martonoș, C.; Oana, L.I. Comparative assessment of contact osteogenesis at the titanium implant–bone junction in male rabbits with dissimilar femoral defects. *Int J Morphol* **2023**, *41*(5), 1317–1322. DOI:10.4067/S0717-95022023000501317 WOS:001145205400033
10. Duma, V.; Ober, C.; Gherman (Dragomir), M.F.; Irimie, A.; Rațiu, C.; Miclăuș, V.; Bogdan, A.; Oana, L. Morphometric evaluation of periosteal and endosteal osseous proliferation around titanium screws inserted using two different pilot hole diameters in the femur of male rabbits. *Rev Rom Med Vet* **2025**, *35*(1), 29–34. WOS:001145205400033
11. Fernea, B.; Damian, A.; Miclăuș, V.; Crișan, M.; Coroian, A.; Martonoș, C.O.; Rațiu, C.; Pece, O.A. Comparative evaluation of osseointegration of titanium screws in rabbits according to sex and physiological status. *Rev Rom Med Vet* **2025**, *35*(1), 35–39. WOS:001478172900006

CVJ CLUJ VETERINARY JOURNAL

Research article

Symmetric Dimethylarginine (SDMA) as a Predictor of Anemia in Early Canine Kidney Dysfunction

Sherly Leilany [1]*, Sebastian Emmanuel Willyanto [2] and Iwan Willyanto [3]

[1] Research and Development Division, INI Veterinary Service, Surabaya 60293, Indonesia; sherly.leilany@gmail.com
[2] Bachelor Study Program of Medicine, Faculty of Medicine, Universitas Brawijaya, Malang 65145, Indonesia; realsebastianemmanuel@gmail.com
[3] Senior Attending Veterinarian, INI Veterinary Service, Surabaya 60293, Indonesia; iwan.willyanto@gmail.com
* Correspondence: Sherly Leilany, sherly.leilany@gmail.com

Abstract: Traditional markers such as creatinine and BUN have limited sensitivity for detecting early kidney dysfunction, whereas symmetric dimethylarginine (SDMA) offers a more reliable indication of reduced glomerular filtration rate. Chronic kidney disease (CKD) in dogs is often associated with anemia due to decreased erythropoietin production, but the relationship between SDMA levels and anemia severity remains unclear. This retrospective cross-sectional study analyzed canine patients presented to INI Veterinary Service, Surabaya, Indonesia, between January 2024 and August 2025, with available complete blood counts and renal function profiles including SDMA, creatinine, and hematocrit (HCT). Anemia severity was classified by HCT values, renal dysfunction was staged according to IRIS criteria, and statistical analyses included Chi-square testing, regression modeling, and ROC curve analysis. Among 157 dogs, anemia was present in 28.2% of cases and increased in prevalence and severity with advancing CKD stage. SDMA concentrations were significantly higher in dogs with severe anemia, yet regression analysis revealed that SDMA, creatinine, and age were not independent predictors of anemia severity. ROC analysis showed moderate discriminatory ability of SDMA (AUC 0.666), with high specificity (81.2%) but limited sensitivity (56.8%). In conclusion, anemia in dogs was more frequent and severe in advanced CKD, but SDMA was not an independent predictor after adjusting for creatinine and age. While ROC analysis suggests SDMA may serve as a supportive "rule-in" biomarker, it lacks sensitivity to function as a standalone diagnostic tool.

Keywords: *symmetric dimethylarginine; anemia; chronic kidney disease; creatinine; canine*

Received:14.09.2025
Accepted:02.12.2025
Published:04.03.2026

DOI:10.52331/v31i1gy09

1. Introduction

The kidney plays a central role in maintaining homeostasis by regulating fluid, electrolyte, acid-base, glucose, protein, lipid, and ion balances, as well as removing metabolic waste [1,2]. Serum creatinine and blood urea nitrogen (BUN) are traditional biomarkers widely used in clinical practice to assess kidney function. However, their sensitivity and specificity are limited, as they are influenced by multiple factors unrelated to kidney function, including age, sex, muscle mass, diet, and certain medications. Moreover, alterations in serum creatinine and BUN are subtle and may not be readily detectable during the early stages of kidney dysfunction [3,4].

Symmetric dimethylarginine (SDMA) is a methylated derivative of the amino acid arginine, produced during protein turnover and released into the bloodstream. It is primarily eliminated by the kidneys through glomerular filtration, with minimal influence from muscle mass, age, or sex. Because SDMA is almost exclusively excreted by the kidneys, its blood concentration rises as glomerular filtration rate (GFR) declines. SDMA increases in the blood with even mild reductions in GFR, often before serum creatinine rises [5,6]. In dogs, SDMA can detect as little as a 20–25% decrease in GFR, making it a highly sensitive early marker of kidney dysfunction [7].

The decline of kidney function and anemia are closely linked, especially in chronic kidney disease (CKD). The kidneys normally produce erythropoietin (EPO), a critical hormone that stimulates red blood cell production [8]. In CKD, however, damaged kidneys lose the ability to produce adequate EPO, resulting in normochromic-normocytic anemia that progressively worsens as kidney function declines [9,10]. Anemia is not only highly prevalent among CKD patients, but also contributes significantly to poorer prognosis and reduced quality of life. It is strongly linked to faster progression to end-stage renal disease, higher rates of cardiovascular events, and elevated all-cause mortality. Therefore, the early identification and management of anemia are essential for improving outcomes in CKD patients [11,12].

In this context, the detection of early or subclinical kidney dysfunction becomes particularly important, as it may enable the recognition of anemia before significant renal damage occurs. SDMA, as previously highlighted, is recognized as a more sensitive biomarker for detecting early kidney dysfunction compared to creatinine [13]. An elevation in SDMA despite normal creatinine values suggests the presence of early or subclinical renal impairment, which could represent a critical window for intervention. However, the association between SDMA-detected early dysfunction and the risk of developing anemia has not yet been clearly established, underscoring the need for further investigation. In response of the current research gap, this study seeks to characterize anemia patterns across early and advanced stages of renal dysfunction in canines by evaluating hematologic and kidney function biomarkers.

The early detection of anemia allows earlier intervention, which can improve patient outcomes and reduce complications. In cases of early or subclinical kidney dysfunction, supportive therapy may help prevent the development of anemia. Moreover, the use of SDMA for early anemia detection could refine CKD staging and patient monitoring. These insights highlight not only their significance in veterinary medicine but also potential parallels in human nephrology.

2. Materials and Methods

2.1 Study Design and Setting

A retrospective cross-sectional research design was used to determine the role of SDMA as a predictor of anemia in early canine kidney dysfunction. The population consisted of canine patients who were hospitalized or seen as outpatients at INI Veterinary Service, Surabaya, Indonesia, between January 2024 and August 2025, and in whom complete blood count (CBC) and renal function tests had been conducted.

2.2 Participants

The inclusion criteria were canine patients presented to INI Veterinary Service, Surabaya, Indonesia, between January 2024 and August 2025, who underwent blood work that included SDMA, HCT, and creatinine measurements obtained during the same clinical encounter. Only cases with complete data sets, measured on standardized analyzers (IDEXX Catalyst One and ProCyte One), were included. The exclusion criteria included: (1) poor sample quality or analyzer flags that could invalidate measurements (marked hemolysis, lipemia, or icterus); (2) evidence of acute kidney injury or clearly prerenal azotemia at the time of sampling (e.g., dehydration/hypovolemia, urinary obstruction), as defined in the medical record; (3) known non-renal causes of anemia (e.g., acute hemorrhage or recent surgery/trauma, gastrointestinal bleeding, hemolysis, hemoparasitosis such as *Babesia*/*Ehrlichia*, severe systemic infection/inflammation, or neoplasia affecting red cell mass); (4) prior blood transfusion within 30 days; or (5) recent therapy that directly alters erythropoiesis (erythropoiesis-stimulating agents, iron/B12/folate supplementation) within the preceding 14–30 days. The independent variable was the SDMA concentration, while the dependent variable was anemia severity, categorized into five levels (normal, mild, moderate, severe, very severe) according to HCT values. Potential confounding variables included patients' age, sex, breed or body size, hydration status, concurrent diseases, and medications that may influence kidney function or red blood cell levels.

2.3 Data Collection

2.3.1 Clinical Data

Demographic and clinical information recorded for each patient included name, sex, age, date of testing, and body weight. Laboratory data consisted of renal function markers (SDMA, creatinine, blood urea nitrogen, and phosphorus) and CBC parameters, including HCT.

2.3.2 Laboratory Assessment

The data were collected by the attending veterinarians responsible for each patient. Blood samples were obtained via venipuncture and placed in EDTA tubes for hematological analysis, while serum samples were

processed for biochemical evaluation. Hematological parameters were measured using the IDEXX ProCyte One hematology analyzer, and biochemical markers, including creatinine and SDMA, were assessed using the IDEXX Catalyst One chemistry analyzer. All reference ranges applied were those validated for canine patients.

2.3.3 Early and Advanced Renal Dysfunction Grouping

Subjects were categorized into four groups according to SDMA and creatinine levels, in line with the 2023 IRIS CKD staging system. The normal group had SDMA levels of 0–14 μg/dL and creatinine levels of 0.5–1.4 mg/dL. The early renal dysfunction group (Stage 1) was defined by SDMA levels of 15–17 μg/dL with creatinine levels remaining at 0.5–1.4 mg/dL. Moderate renal dysfunction (Stage 2) included subjects with SDMA levels between 18–35 μg/dL and creatinine levels of 1.4–2.8 mg/dL. The advanced renal dysfunction group (Stages 3 and 4) was characterized by SDMA levels ≥36 μg/dL and creatinine levels ≥2.9 mg/dL [14].

2.3.4 Anemia Severity Grouping

The analysis categorized canine patients into groups based on the severity of anemia. Classification was determined using HCT values, with anemia defined as HCT <37%. Severity was further stratified into the following categories: mild anemia (HCT 30–36.9%), moderate anemia (HCT 20–29.9%), severe anemia (HCT 13–19.9%), and very severe anemia (HCT < 13%). Dogs with HCT ≥ 37% were classified as having no anemia [15].

2.4 Statistical Analysis

Data were analyzed using IBM SPSS Statistics (version 31, IBM Corp., Armonk, NY). Descriptive statistics were reported as mean ± standard deviation (SD) or median (interquartile range, IQR) for continuous variables, and frequency (percentage) for categorical variables. Comparisons of anemia severity (normal, mild, moderate, severe, very severe) across renal dysfunction stages (normal, early, moderate, advanced) were performed using the Chi-square test for trend. Differences in SDMA and hematocrit (HCT) levels across anemia severity groups were evaluated using one-way ANOVA or the Kruskal–Wallis test, depending on data distribution, followed by appropriate post hoc tests. Correlation between SDMA and HCT values was assessed using Pearson's or Spearman's correlation coefficients. To explore the relationship between SDMA and anemia severity, an ordinal logistic regression model was applied with anemia severity (five categories) as the dependent variable and SDMA as the independent predictor, adjusting for potential confounders such as age, sex, and creatinine. Receiver operating characteristic (ROC) curve analysis was additionally performed to assess the discriminatory performance of SDMA for detecting clinically relevant anemia (defined as HCT <37%). A two-sided p-value <0.05 was considered statistically significant.

2.5 Ethical Considerations

This study was based on a retrospective review of canine patient records. All blood samples were collected as part of routine clinical diagnostic procedures, and no additional samples were drawn for research purposes. Informed consent for blood collection and diagnostic testing had been obtained from the owners by the attending veterinarians at the time of clinical evaluation. Patient confidentiality was maintained throughout the study by anonymizing identifying information such as name and medical record number. Ethical approval for the use of clinical data was obtained from INI Veterinary Service, Surabaya, Indonesia, in accordance with guidelines for the ethical use of animals in research (Protocol No. IACUC-INIVET-2025-001).

3. Results

3.1 Study Population and Baseline Characteristics

A total of 173 blood test results were initially collected, but cases without creatinine values were excluded. After this adjustment, 157 canine patients were included in the analysis. Among them, 60.5% were female. The dogs had a mean age of 10 years (range: 1–17 years) and a mean body weight of 19.9 lbs (range: 2.4–79.4 lbs). The data were collected between January 2024 and August 2025. Detailed baseline characteristics are presented in **Appendix A**.

3.2 Frequencies of CKD Staging and Anemia

A total of 157 canine patients were included in the analysis. Most patients had normal hematocrit values (71.8%), while mild (13.4%), moderate (8.3%), severe (2.5%), and very severe (3.8%), where anemia was less common. This distribution of data indicates that anemia severity was toward the non-anemic group,

with only a minority of patients experiencing anemia. Based on the IRIS classification, nearly half of the dogs (49.7%) were classified as having early CKD, 30.6% as moderate, 8.3% as advanced, and 11.5% showed normal renal function. Thus, the majority of cases are presented in the early to moderate stages of disease.

3.3 Relationship between CKD stage and Anemia Severity

Chi-square analysis **(Table 1)** indicated a significant association between CKD stage and anemia severity ($\chi^2 = 28.4$, df = 12, p = 0.005). However, more than 60% of the expected cell counts were <5, limiting the reliability of the result. Despite this limitation, descriptive trends were observed. Patients with advanced CKD showed the highest proportion of anemia (54%), compared to moderate CKD (42%), early CKD (17%), and those without CKD (22%). Mild to moderate anemia was most commonly found in patients with early and moderate CKD, while severe and very severe anemia was uncommon and appeared primarily in advanced CKD stages. Notably, a few individuals without CKD also presented with very severe anemia, indicating that anemia can develop from causes unrelated to CKD.

Table 1. Chi-square analysis on the relationship between CKD stage and anemia severity.

		Anemia Severity Classification					**Total**
		Mild	Moderate	Normal	Severe	Very Severe	
CKD IRIS[1] Classification	Normal	1	1	14	0	2	18
	Moderate	9	8	28	2	1	48
	Early	8	3	65	0	2	78
	Advanced	3	1	6	2	1	13
	Total	21	13	113	4	6	157

[1] Chronic Kidney Disease-International Renal Interest Society

3.4 SDMA levels across anemia categories

The Kruskal–Wallis test **(Fig. 1)** demonstrated significant differences in SDMA across anemia categories (H = 18.3, df = 4, p = 0.001). Post-hoc analysis revealed that only the severe anemia group differed significantly from the normal group after Bonferroni adjustment (p = 0.031). Descriptively, SDMA concentrations were lowest in the normal and very severe anemia groups, intermediate in mild and moderate anemia, and highest in severe anemia. The severe anemia category also showed the widest variability, with several markedly elevated values (>70 μg/dl), suggesting heterogeneity of renal dysfunction within this group. Interestingly, patients with very severe anemia demonstrated relatively low and clustered SDMA values, which may reflect small sample size or anemia from non-renal etiologies. Outliers were also noted in the normal group, indicating that elevated SDMA can occur even in the absence of anemia. Overall, these findings suggest that SDMA elevations become most apparent in association with severe anemia, whereas mild to moderate anemia may not consistently reflect underlying renal impairment.

3.5 Ordinal Logistic Regression on Predictors for Anemia Severity and CKD Staging

Ordinal logistic regression using anemia severity as the dependent variable showed that SDMA (p = 0.477), creatinine (p = 0.871), and age (p = 0.120) were not significant predictors. The model did not significantly improve fit compared with the intercept-only model ($\chi^2 = 3.88$, p = 0.275), indicating that anemia severity was not explained by these variables. In contrast, ordinal regression with CKD stage as the outcome demonstrated a significant overall model fit ($\chi^2 = 38.9$, $p < 0.001$; Nagelkerke $R^2 = 0.245$), with creatinine emerging as a significant predictor (B = −0.837, p = 0.010). SDMA and age were not significant. Goodness-of-fit statistics (Pearson $\chi^2 = 341.3$, p = 0.999) indicated adequate model fit. These findings suggest that while creatinine is strongly associated with CKD stage, neither creatinine, SDMA, nor age predicted anemia severity, underscoring the importance of direct hematologic assessment in CKD patients.

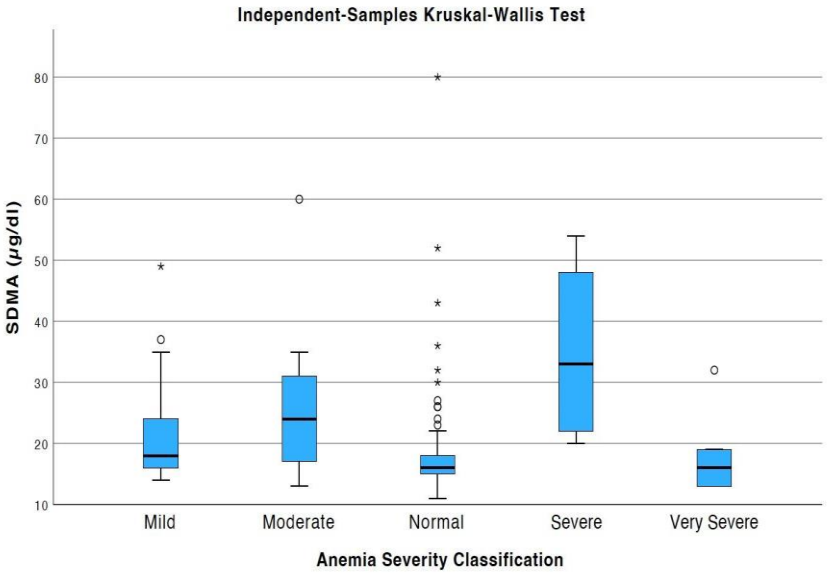

Figure 1. Kruskal–Wallis test on SDMA levels across anemia severity categories. The blue boxes represent the interquartile range (IQR), with the horizontal line inside each box indicating the median SDMA concentration. The whiskers extend to the minimum and maximum values within 1.5 × IQR, while circles and asterisks denote outliers and extreme values, respectively.

3.6 ROC Curve Analysis

ROC analysis for detection of clinically relevant anemia (≥ mild) showed that SDMA had moderate discriminatory ability (AUC = 0.666, 95% CI 0.560–0.773, p = 0.002), whereas creatinine demonstrated poor and insignificant performance (AUC = 0.592, p = 0.118) **(Fig. 2)**. The optimal SDMA cutoff of 18.5 µg/dL provided 56.8% sensitivity and 81.2% specificity, yielding a Youden index of 0.381. In contrast, the optimal creatinine cutoff of 1.35 mg/dL resulted in lower sensitivity (45.5%) but similar specificity (87.5%), with a Youden index of 0.330 **(Table 2).** These findings indicate that SDMA is more reliable than creatinine for identifying anemia associated with renal dysfunction, particularly due to its higher discriminatory ability and good specificity. However, the modest sensitivity of SDMA suggests that normal or near-normal values do not exclude the presence of anemia, underscoring the need for SDMA to be interpreted alongside other clinical and laboratory parameters.

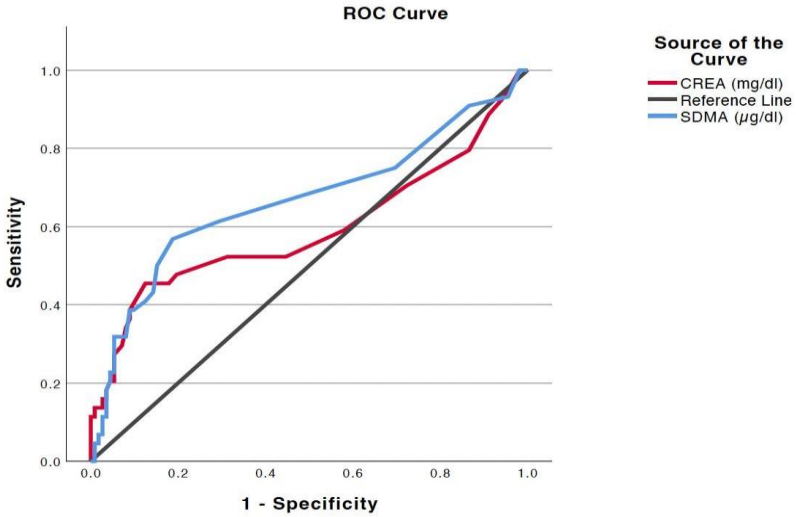

Figure 2. Receiver operating characteristic (ROC) curve with binormal smoothing for the detection of clinically relevant anemia. The light blue line represents the creatinine, the cyan line represents SDMA, and the diagonal magenta line represents the reference line for a non-discriminatory test.

Table 2. The optimal cutoff, sensitivity, 1-specificity, and Youden index of SDMA and creatinine in detecting clinically significant anemia.

	Parameter			
Biomarkers	Optimal Cutoff	Sensitivity	1-Specificity	Youden Index
SDMA	18.50	0.568	0.188	0.381
Creatinine	1.350	0.455	0.125	0.330

4. Discussion

The results of this study indicate that anemia becomes more prevalent and severe with advancing CKD stage, consistent with prior reports that link renal dysfunction to impaired erythropoietin production and chronic inflammation. As kidney function declines, the ability to produce erythropoietin, the hormone that stimulates red blood cell production diminishes, leading to reduced erythroid precursor cells in the bone marrow and worsening anemia [8]. In the study by Lippi et al. (2021), anemia was reported in approximately 60% of dogs, with the highest prevalence observed in the more advanced CKD IRIS stages. The frequency of anemia increased particularly in dogs with CKD IRIS stages 3 and 4, in which the frequency exceeded 70% [15]. In dogs with CKD, anemia prevalence rises from 47% in IRIS stage 2, to 71% in stage 3, and 82% in stage 4. Severity also increases, with moderate to severe anemia more common to be found in later stages. Morphological abnormalities in red blood cells, such as anisocytosis and poikilocytosis, become more frequent as CKD progresses, indicating worsening bone marrow function [15,16]. Although the chi-square test supported an association between CKD stage and anemia, the uneven distribution of cases across categories limited statistical robustness.

Gunawan et al. (2023) reported a dog with IRIS stage 4 CKD that exhibited severe non-regenerative anemia in conjunction with a markedly elevated SDMA concentration (64 μg/dL; reference range: 0–14 μg/dL) [17]. This suggests that dogs with severe anemia due to advanced kidney disease can have significantly increased SDMA concentrations. SDMA levels were higher in dogs with severe anemia compared with non-anemic dogs, suggesting that progressive renal impairment is associated with anemia severity. Aging itself is associated with mild decreases in hematocrit and serum iron, likely due to iron-restricted erythropoiesis and low-grade inflammation, but these changes are less pronounced than those seen with significant renal dysfunction [18]. Therefore, this relationship was not consistent across all anemia categories, likely due to the small sample size in severe groups.

Ordinal logistic regression failed to demonstrate SDMA as an independent predictor of anemia severity after adjusting for creatinine and age. In contrast, creatinine was strongly associated with CKD stage, reaffirming its established role as a renal biomarker. These findings suggest that while SDMA reflects renal dysfunction, it may not directly drive the pathogenesis of anemia.

ROC curve analysis demonstrated that SDMA had a moderate discriminatory capacity for identifying clinically relevant anemia, with an optimal cutoff of 18.5 μg/dL. At this threshold, specificity was relatively high (81.2%), but sensitivity was modest (56.8%). This performance profile suggests that SDMA may be more useful as a "rule-in" test for anemia associated with renal dysfunction, as elevated values strongly support the presence of disease, whereas normal or near-normal values do not reliably exclude it.

The superior performance of SDMA compared to creatinine (AUC 0.666 vs. 0.592, respectively) is consistent with its known ability to detect renal impairment earlier and more reliably than creatinine, which is strongly influenced by factors such as muscle mass, hydration status, and extrarenal conditions [19,20]. The moderate, but not excellent, discriminative capacity observed in this study indicates that SDMA alone should not be considered a definitive diagnostic tool for anemia in CKD but rather a complementary biomarker to be interpreted alongside hematological indices (HCT, reticulocyte count), renal staging, and iron status.

Importantly, the relatively high specificity observed for SDMA suggests that its greatest clinical utility may lie in identifying subsets of dogs where anemia is more likely to be of renal origin. This may help differentiate CKD-related anemia from anemia due to other etiologies such as nutritional deficiencies, chronic inflammation, or bone marrow disorders. On the other hand, the limited sensitivity underscores the need for caution, as relying solely on SDMA could result in underdiagnosis of clinically relevant anemia, particularly in earlier CKD stages or when multiple factors contribute to anemia development.

Taken together, these results highlight the potential utility of SDMA in the clinical evaluation of dogs with CKD. While SDMA may not serve as a strong independent predictor of anemia severity, it demonstrates

moderate diagnostic accuracy and outperforms creatinine in identifying clinically meaningful anemia. Larger, balanced cohorts are needed to validate the cutoff identified in this study and to clarify the role of SDMA in the complex interplay between renal dysfunction and anemia in canine patients.

5. Conclusions

In conclusion, both the prevalence and the morphological abnormalities of anemia in dogs increase progressively with advancing IRIS stages. Although SDMA concentrations were elevated in dogs with more advanced CKD and severe anemia, multivariable analysis did not establish SDMA as an independent predictor of anemia severity after accounting for creatinine and age. Nevertheless, ROC curve analysis indicated that SDMA has a moderate discriminatory ability for detecting clinically relevant anemia, with relatively high specificity but limited sensitivity. These findings suggest that SDMA may serve as a useful adjunctive biomarker in the clinical evaluation of dogs with CKD, particularly as a supportive "rule-in" test to identify anemia of renal origin, but should not replace conventional hematological and biochemical assessments. Further studies with larger and more balanced populations are warranted to validate the diagnostic thresholds and better define the clinical role of SDMA in the early recognition and management of CKD-associated anemia in dogs.

Author Contributions: Conceptualization, S.L.; Methodology, S.L.; Formal analysis, S.L. and S.E.W. (statistical analysis); Investigation, S.L. and S.E.W.; Resources, I.W.; Data curation, S.L. and S.E.W.; Writing—original draft preparation, S.L. and S.E.W.; Writing—review and editing, I.W.; Supervision, I.W.; Project administration, S.L.; Clinical oversight and case verification, I.W. All authors have read and agreed to the published version of the manuscript.

Funding: This research received no external funding.

Institutional Review Board Statement: The study was conducted according to the guidelines for the care and use of animals, and approved by the Institutional Animal Care and Use Committee (IACUC) of INI Veterinary Service (Protocol No. IACUC-INIVET-2025-001). Informed consent was obtained from the dog owners prior to inclusion of their animals in the study.

Data Availability Statement: The data supporting this study are derived from hospital/clinical records and contain sensitive information. Therefore, they are not publicly available but may be provided by the corresponding author upon reasonable request.

Acknowledgments: The authors would like to thank the veterinary staff of INI Veterinary Service for their assistance in data collection and case management.

Conflicts of Interest: The authors declare no conflict of interest.

References

1. Borin-Crivellenti, S.; Crivellenti, L.Z.; Gilor, C.; Gilor, S.; Silva, D.G.; Maia, S.R.; Costa, P.B.; Alvarenga, A.W.; Fernandes, A.L.; Santana, A.E. Anemia in canine chronic kidney disease is multifactorial and associated with decreased erythroid precursor cells, gastrointestinal bleeding, and systemic inflammation. *Am J Vet Res* **2023**, *84*, 1–6. DOI: 10.2460/ajvr.23.05.0097.
2. Cernaro, V.; Coppolino, G.; Visconti, L.; Rivoli, L.; Lacquaniti, A.; Santoro, D.; Buemi, A.; Loddo, S.; Buemi, M. Erythropoiesis and chronic kidney disease–related anemia: From physiology to new therapeutic advancements. *Med Res Rev* **2019**, *39*, 427–460. DOI: 10.1002/med.21527.
3. Clase, C.M.; Carrero, J.J.; Ellison, D.H.; Grams, M.E.; Hemmelgarn, B.R.; Jardine, M.J.; Kovesdy, C.P.; Kline, G.A.; Lindner, G.; Obrador, G.T.; Palmer, B.F. Potassium homeostasis and management of dyskalemia in kidney diseases: conclusions from a KDIGO Controversies Conference. *Kidney Int* **2020**, *97*, 42–61. DOI: 10.1016/j.kint.2019.09.018.
4. Gunawan, M.; Amelia, F.; Resyana, N.N.; Zulfaichsanniyati, R.C.; Zaenab, S.; Widyaputri, T. IRIS-stage 4 CKD in a dog: diagnostic approaches and staging of chronic kidney disease: a case study. *J Exp Biol Agric Sci* **2023**, *11*, 216–225. DOI: 10.18006/2023.11(1).216.225.
5. Hamza, E.; Metzinger, L.; Metzinger-Le Meuth, V. Uremic toxins affect erythropoiesis during the course of chronic kidney disease: a review. *Cells* **2020**, *9*, 2039. DOI: 10.3390/cells9092039.
6. Hanna, R.M.; Streja, E.; Kalantar-Zadeh, K. Burden of anemia in chronic kidney disease: beyond erythropoietin. *Adv Ther* **2021**, *38*, 52–75. DOI: 10.1007/s12325-020-01524-6.
7. Imenez Silva, P.H.; Mohebbi, N. Kidney metabolism and acid–base control: back to the basics. *Pflugers Arch* **2022**, *474*, 919–934. DOI: 10.1007/s00424-022-02696-6.
8. International Renal Interest Society (IRIS). IRIS Staging of CKD (modified 2023). *IRIS Kidney* **2023**. Available online: https://www.iris-kidney.com (accessed on August 25, 2025).
9. Kashani, K.; Rosner, M.H.; Ostermann, M. Creatinine: from physiology to clinical application. *Eur J Intern Med* **2020**, *72*, 9–14. DOI: 10.1016/j.ejim.2019.10.025.

10. Khairat, A.S.; Harun, H.; Viotra, D. Symmetric Dimethylarginine as a Biomarker for Chronic Kidney Disease. *Bioscientia Med* **2023**, *7*, 3602–3608. DOI: 10.37275/bsm.v7i9.866.
11. Lippi, I.; Perondi, F.; Ghiselli, G.; Santini, S.; Habermaass, V.; Marchetti, V. Anemia in dogs with acute kidney injury. *Vet Sci* **2024**, *11*, 212. DOI: 10.3390/vetsci11050212.
12. Nabity, M.B.; Lees, G.E.; Boggess, M.M.; Yerramilli, M.; Obare, E.; Yerramilli, M.; Rakitin, A.; Aguiar, J.; Relford, R. Symmetric dimethylarginine assay validation, stability, and evaluation as a marker for the early detection of chronic kidney disease in dogs. *J Vet Intern Med* **2015**, *29*, 1036–1044. DOI: 10.1111/jvim.12835.
13. Portolés, J.; Martín, L.; Broseta, J.J.; Cases, A. Anemia in chronic kidney disease: from pathophysiology and current treatments, to future agents. *Front Med* **2021**, *8*, 642296. DOI: 10.3389/fmed.2021.642296.
14. Radakovich, L.B.; Pannone, S.C.; Truelove, M.P.; Olver, C.S.; Santangelo, K.S. Hematology and biochemistry of aging—evidence of "anemia of the elderly" in old dogs. *Vet Clin Pathol* **2017**, *46*, 34–45. DOI: 10.1111/vcp.12459.
15. Relford, R.; Robertson, J.; Clements, C. Symmetric dimethylarginine: improving the diagnosis and staging of chronic kidney disease in small animals. *Vet Clin N Am Small Anim Pract* **2016**, *46*, 941–960. DOI: 10.1016/j.cvsm.2016.06.010.
16. Rysz, J.; Gluba-Brzózka, A.; Franczyk, B.; Jabłonowski, Z.; Ciałkowska-Rysz, A. Novel biomarkers in the diagnosis of chronic kidney disease and the prediction of its outcome. *Int J Mol Sci* **2017**, *18*, 1702. DOI: 10.3390/ijms18081702.
17. Siwinska, N.; Zak, A.; Slowikowska, M.; Niedzwiedz, A.; Paslawska, U. Serum symmetric dimethylarginine concentration in healthy horses and horses with acute kidney injury. *BMC Vet. Res* **2020**, *16*, 396. DOI: 10.1186/s12917-020-02621-y.
18. Szlosek, D.; Robertson, J.; Quimby, J.; Mack, R.; Ogeer, J.; Clements, C.; McCrann, D.J.; Coyne, M.J. A retrospective evaluation of the relationship between symmetric dimethylarginine, creatinine and body weight in hyperthyroid cats. *PLoS ONE* **2020**, *15*, e0227964. DOI: 10.1371/journal.pone.0227964.
19. Taderegew, M.M.; Wondie, A.; Terefe, T.F.; Tarekegn, T.T.; GebreEyesus, F.A.; Mengist, S.T.; Amlak, B.T.; Emeria, M.S.; Timerga, A.; Zegeye, B. Anemia and its predictors among chronic kidney disease patients in Sub-Saharan African countries: a systematic review and meta-analysis. *PLoS ONE* **2023**, *18*, e0280817. DOI: 10.1371/journal.pone.0280817.
20. Wasung, M.E.; Chawla, L.S.; Madero, M. Biomarkers of renal function, which and when? *Clin Chim Acta* **2015**, *438*, 350–357. DOI: 10.1016/j.cca.2014.08.039.

CVJ CLUJ VETERINARY JOURNAL

Research article

Spectrofluorimetric investigations of urine in cats diagnosed with renal disorders

Mariana Tătaru [1*], Alina Rotărescu [2], Radu Lăcătuș [1], Cristiana Novac [1] and Ionel Papuc [1]

[1] University of Agricultural Sciences and Veterinary Medicine, Faculty of Veterinary Medicine, Manastur 3-5 Street, Cluj-Napoca, Cluj, Romania; mariana.tataru@usamvcluj.ro; radu.lacatus@usamvcluj.ro; cristiana.novac@usamvcluj.ro; ionel.papuc@usamvcluj.ro
[2] R&D FARMA ZOO MED SRL, King Ferdinand Square I 8 Street, Loc. Medias, Sibiu, Romania; alina.rotarescu@yahoo.com
* Correspondence: mariana.tataru@usamvcluj.ro; Tel.: 0743133890

Abstract: Laboratory investigations are essential for establishing an accurate diagnosis in veterinary medicine; however, urinalysis in feline urinary tract pathology is often underestimated, despite its important role in determining etiology and monitoring therapy. This study reemphasizes the importance of urinalysis in cats with renal disorders and proposes urine spectrofluorometry as an innovative method for etiological diagnosis. The aim of this study was to reemphasize the importance of urinalysis in cats diagnosed with renal disorders and to propose urine spectrofluorometry as a novel laboratory method for the etiological diagnosis of these.
In the spectrofluorimetric examination, emission spectra were obtained by exciting urine samples at wavelengths of 280 nm and 400 nm, focusing on the presence of tryptophan fluorophore metabolites. Comparative analysis of emission band intensities revealed significant differences between urine from healthy cats and urine from cats diagnosed with urinary tract disorders. Spectrofluorimetric analysis of urine allows the identification of specific renal biochemical alterations by observing variations in the emission band intensities characteristic of tryptophan metabolites. The results indicate a decrease in fluorescence intensity at λ_ex = 280 nm in healthy cats and an increase at λ_ex = 400 nm in cats with urinary infections and renal impairment, thus confirming the potential of this laboratory method as a rapid, non-invasive, and sensitive diagnostic tool for establishing the etiology of the disease.

Keywords: spectrofluorimetry, urine, cats, renal disorders, tryptophan, fluorophores

1. Introduction

In veterinary medicine, urinalysis is sometimes treated superficially or, in many cases, even ignored, even though this examination can provide crucial information for determining disease etiology or monitoring instituted therapy. A major focus of researchers worldwide has been, and continues to be, the development of non-invasive, reliable, and cost-effective methods for investigating renal diseases and monitoring health status in both animals and humans [1,2]. Fluorescence spectroscopy is considered a potential tool for investigating various systemic disorders, and due to qualities such as sensitivity, specificity, and non-invasiveness, it can be regarded as a complementary technique for diagnosing multiple conditions, including renal diseases [3]. This technique allows the investigation of numerous tissues and biological fluids. In this study, urine was used as the biological fluid of interest, primarily due to its ease of collection and high content of metabolites, including tryptophan metabolites and native fluorophores [4,5]. Because of these metabolites, urine fluorescence can serve as a laboratory method for diagnosing a wide range of conditions, such as proteinuria, nephritic syndrome, hepatopathy, lipofuscinosis, or neuronal ceroid lipofuscinosis [6]. Renal disorders and urinary tract infections in cats represent a common problem in veterinary medicine, significantly affecting quality of life and the prognosis of various pathologies.

Received: 14.11.2025
Accepted: 04.03.2026
Published: 05.03.2026
DOI10.52331/V31i1h812

Classical paraclinical diagnostic methods, based on biochemical and microscopic urine analysis, can be complemented by modern spectroscopic techniques. Spectrofluorimetry is a sensitive laboratory technique based on the property of certain biological compounds to emit fluorescent radiation upon excitation with ultraviolet or visible light. In biological fluids, the most important endogenous fluorophores are derivatives of tryptophan, tyrosine, and NADH (Reduced Nicotinamide Adenine Dinucleotide) [7,8]. The objective of this study was to evaluate the spectral differences between urine samples from healthy cats and those from cats with renal disorders, by highlighting variations in emission band intensities specific to tryptophan metabolites.

Fluorescence spectroscopy is a highly sensitive analytical technique used to characterize the biochemical composition of tissues and biological fluids, providing semi-quantitative information on the distribution of endogenous or exogenous fluorophores [7]. The principle of the method is based on the interaction between electromagnetic radiation and matter, particularly within the UV–VIS (<700 nm) and NIR (700–900 nm) ranges, generating phenomena such as absorption, emission, and scattering [9].

The fluorescence phenomenon is characterized by a red shift of the emission wavelength relative to the excitation wavelength, caused by non-radiative transitions, as well as by the independence between the emission and excitation wavelengths. The fluorescence spectrum of a molecule is generally the mirror image of its absorption spectrum [10]. The main parameters that define the fluorescent properties of a molecule are the quantum yield, the ratio between emitted and absorbed photons, and the fluorescence lifetime, which represents the average time a molecule remains in the excited state [10]. This method allows the analysis of fluorescence differences between amino acids within protein structures and the evaluation of urinary metabolites, proving useful in identifying biochemical changes associated with renal pathological processes [11]. Therefore, fluorescence spectroscopy represents a valuable tool in metabolomics, capable of highlighting alterations in metabolite profiles under physiological or pathological conditions [10,12].

The fluorescence process involves three successive stages: excitation, relaxation, and emission, which reflect the energetic transformations of fluorophores following interaction with electromagnetic radiation [12]. Emission spectra were obtained using a PerkinElmer LS 55 spectrofluorometer, with sample excitation at two distinct wavelengths: 280 nm for tryptophan metabolites and 400 nm for oxidized aromatic compounds. Spectra were recorded within the 300–600 nm range, and results were expressed according to the maximum height of the emission bands (Imax). Statistical analysis was performed by comparing the mean intensity values between the two groups.

2. Materials and Methods

The study was conducted on 12 adult cats divided into two groups: a control group (n = 6), consisting of clinically healthy cats, and an experimental group (n = 6), including cats diagnosed with renal disorders or urinary tract infections. A total of 12 urine samples (one per animal) were analyzed.

Diagnosis was established based on clinical examination and complementary paraclinical investigations, including hematology, serum biochemistry, and urinalysis.

Urine samples were collected aseptically using sterile 60 mL urine collection containers (manufacturer specified by supplier). Depending on the clinical situation, three collection methods were used: manual expression (abdominal massage), performed by transabdominal palpation in the ventral abdominal region or at the pelvic floor level. Gentle pressure was applied to the caudal pole of the urinary bladder to induce micturition, and urine was collected directly into sterile containers. Litter box collection, a commercial urine collection kit with non-absorbent beads (manufacturer specified by supplier) was used. The litter box was thoroughly cleaned and disinfected before placement of the beads. Urine was collected using a sterile pipette and transferred into sterile containers. Urethral catheterization, performed under general anesthesia using sterile urinary catheters adapted to patient size and sex (manufacturer specified by supplier). The catheter was inserted into the urinary bladder through the urethra, and urine was collected directly into sterile containers. All samples were protected from light exposure and stored at 4°C until analysis.

Analyses were performed immediately or within a short time after collection to minimize biochemical and fluorescent degradation. Routine urine examination was performed using Laboquick Urinalysis Reagent Strips (Laboquick®, manufacturer according to product packaging).

The parameters assessed included pH, specific gravity, protein, glucose, ketones, bilirubin, urobilinogen, nitrites, and leukocytes. Urinary sediment examination was carried out after centrifugation (centrifuge

model and manufacturer to be specified), followed by microscopic evaluation using a light microscope (model and manufacturer to be specified).

Fluorescence analysis was performed using a Jasco FP-8200 (JASCO International Co., Ltd., Tokyo, Japan). Before measurements, the instrument was equilibrated for approximately 30 minutes to allow stabilization of the xenon lamp and electronic components. Wavelength calibration and system verification were performed according to the manufacturer's protocol using certified reference standards. Urine samples were placed in quartz cuvettes with a 1 cm optical path length (manufacturer specified by supplier). Spectral acquisition was conducted at room temperature. Excitation and emission wavelength ranges were selected to detect endogenous fluorophores (e.g., aromatic amino acids and NADH). Each sample was analyzed in duplicate to ensure reproducibility. Background correction was performed using distilled water blanks measured under identical conditions. All procedures were conducted under standardized laboratory conditions to ensure methodological consistency, reliability, and reproducibility of the results.

3. Results

The analysis of fluorescence spectra obtained by exciting the urine samples at 280 nm revealed, in most cases, the presence of three main emission bands located between 390 nm and 620 nm, with variations correlated to the clinical status of each examined cat (Table 1).

Table 1. Analysis of fluorescence spectra obtained by excitation of urine samples at 280 nm.

Group	λex (nm)	λem (nm) – maxim	Mean intensity (Imax ± SD)	Observations
Control	280	340	1520 ± 110	Typical tryptophan spectrum, high intensity
Experimental	280	340	890 ± 95	Significant decrease in intensity ($p < 0.05$)
Control	400	460	720 ± 80	Weak band, oxidized aromatic compounds
Experimental	400	460	1180 ± 105	Marked increase in intensity ($p < 0.01$)

The results obtained highlight clear changes in the fluorescent characteristics of urine in cats with renal disorders. For example, the sample from a cat diagnosed with renal colic (Case 1) exhibited three emission bands at 410 nm, 450 nm, and 520 nm. In the case of the cat diagnosed with a bacterial urinary tract infection (Case 2), the fluorescence spectrum showed three emission bands at 415 nm, 450 nm, and 520 nm (Figure 1). This profile is similar to that of Case 1, but with a slight red shift of the emission maximum, indicating changes in the composition of fluorophores, most likely due to the presence of leukocytes and hemoglobin degradation products in the urine.

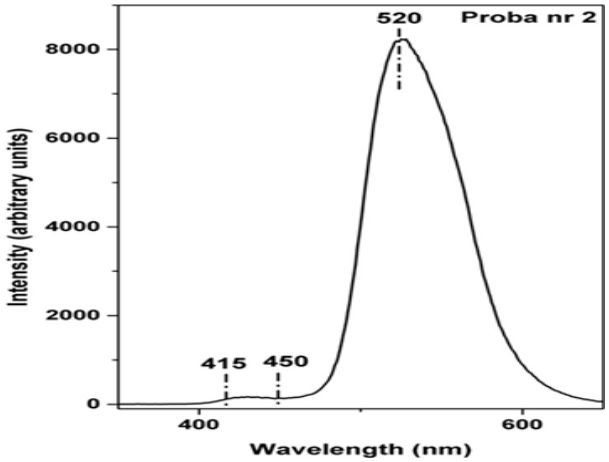

Figure 1. Fluorescence spectrum of the urine sample collected from Case 2

The spectrum of the sample from the cat diagnosed with lower urinary tract disease (Case 3) exhibited emission bands at 390 nm, 450 nm, and 520 nm (Figure 2). This result confirms the involvement of a bacterial infectious process and supports the hypothesis that indolic metabolites can be used as urinary biomarkers for renal disorders and urinary tract infections.

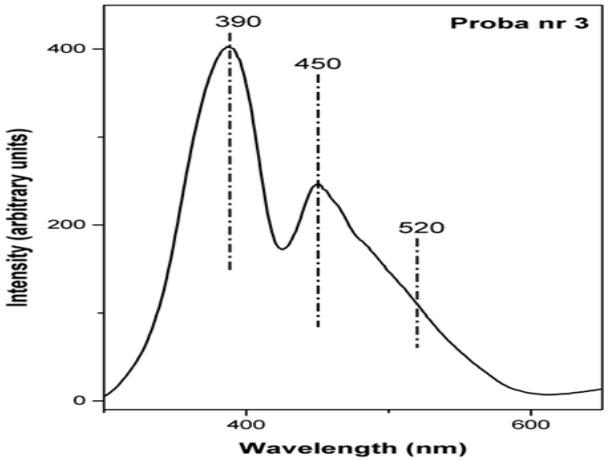

Figure 2. Fluorescence spectrum of the urine sample collected from Case 3

Regarding the cat whose urine was collected by abdominal massage (Case 4), the sample spectrum exhibited emission maxima at 405 nm, 450 nm, and 520 nm (Figure 3). The slight shift of the first band toward longer wavelengths compared to Case 3, suggests a lower concentration of indoxyl compounds, while simultaneously indicating a more pronounced presence of urinary proteins, possibly albumin or cellular enzymes released following renal epithelial damage.

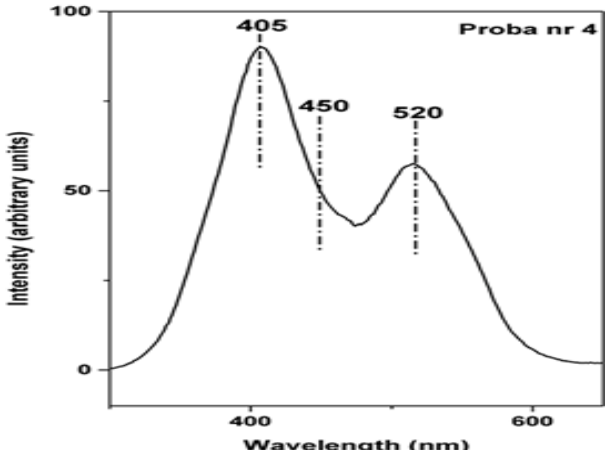

Figure 3. Fluorescence spectrum of the urine sample collected from Case 4

The sample collected from the cat diagnosed with dysuria (Case 5) exhibited three emission bands at 420 nm, 455 nm, and 512 nm (Figure 4). These results suggest the predominance of protein fluorophores, associated with moderate inflammatory activity and the presence of proteinuria. The lower emission wavelengths indicate a simpler composition of fluorophores, with a possible contribution from flavin compounds.

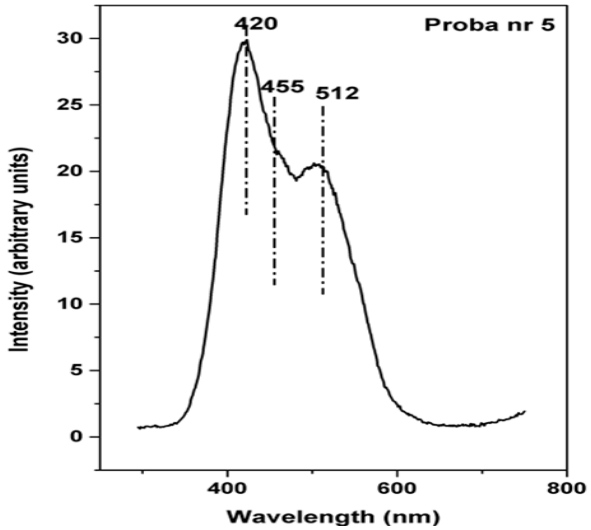

Figure 4. Fluorescence spectrum of the urine sample collected from Case 5

The urine sample from the cat diagnosed with a renal disorder (Case 6) exhibited emission maxima at 474 nm, 560 nm, and 619 nm respectively, indicating a significant red shift of the fluorescence bands.

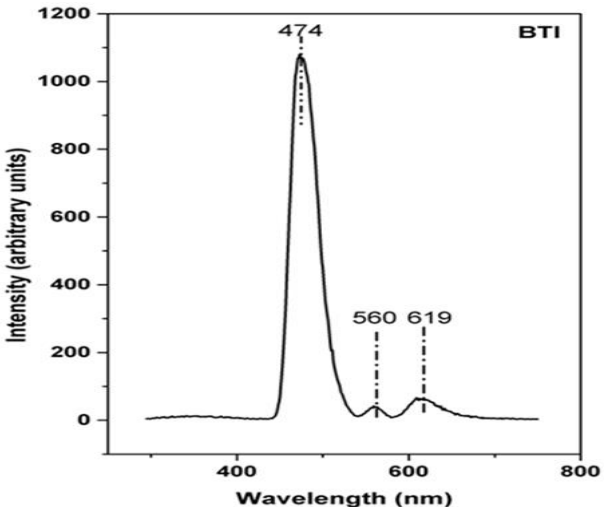

Figure 5. Fluorescence spectrum of the urine sample collected from Case 6

In future studies, the combined analysis of emission spectra with chromatographic and metabolomic methods could allow the precise identification of the compounds responsible for the observed bands and the establishment of specific urinary biomarkers for the early diagnosis of renal diseases in cats. The decrease in the intensity of bands associated with tryptophan (λ ex = 280 nm) may be correlated with reduced excretion of protein metabolites or degradation of fluorescent compounds during pathological processes. In contrast, the increase in intensity at λ_ex = 400 nm suggests the accumulation of oxidized aromatic products, associated with oxidative stress and impaired renal function. These observations confirm the usefulness of spectrofluorimetry as a complementary diagnostic and monitoring tool for renal disorders in cats.

4. Discussion

Assessment of renal function in domestic carnivores typically involves a combination of complementary tests. However, the interpretation of these tests often remains uncertain due to the limited sensitivity of the equipment used, the high biological variability related to species, and the high costs involved. Urinalysis offers numerous benefits, namely: urine serves as a good indicator of certain conditions, making these analyses recommended for monitoring health status; this type of examination can be performed daily, as direct urine collection during micturition does not cause discomfort to the patient; and urinalysis or urine culture

can be performed annually, even in the absence of clinical symptoms, because urinary tract infections are often asymptomatic. Traditional diagnostic methods used in feline renal pathology remain fundamental, yet spectrofluorimetric examination, as a modern diagnostic approach, complements the methodological toolkit and may become a new tool for exploring and monitoring the health status of cats. Urine is recognized as one of the biological fluids with significant fluorescent properties, due to its high concentration of metabolites present in both physiological and pathological states [13]. Fluorescence intensity is not a strictly linear function of fluorophore concentration, being influenced by factors such as self-quenching, energy transfer, and interactions between compounds. Thus, changes in the composition and concentration of fluorophores result in significant variations in the shape and intensity of emission spectra [13]. The literature reports that excitation of urine samples at a wavelength of 290 ± 10 nm induces emission bands associated with fluorophores derived from tryptophan metabolism [14]. Moreover, in the presence of infectious processes, bacteria can produce indoxyl compounds, such as indoxyl sulfate and indoxyl-3-acetate, which exhibit emission maxima around 390 nm [15,16].

These wavelengths mainly correspond to the fluorescence of urinary proteins and tryptophan metabolites. The increased intensity around 450 nm suggests the accumulation of fluorescent aromatic compounds, possibly derivatives of NADH and flavins, which are indicators of oxidative stress and inflammation [10].

The band at 390 nm is particularly significant, as it is associated with the presence of indoxyl compounds, such as indoxyl sulfate and indoxyl-3-acetate, formed as a result of bacterial activity on tryptophan [14,15,17]. This variation is observed when there is an accumulation of bile pigments and oxidized aromatic compounds, suggesting severe renal impairment or an advanced lower urinary tract infection [10,14]. The results obtained clearly demonstrate that fluorescence spectroscopy can be used as a non-invasive method to evaluate biochemical changes in the urine of cats with renal and urinary disorders. Differences in the position and intensity of emission bands reflect variations in metabolic composition and may indicate the presence of infectious or inflammatory processes. The emission spectra obtained in this study are consistent with observations reported in the literature, which associate excitation in the 280–290 nm range with the detection of aromatic fluorophores such as tryptophan, tyrosine, NADH, and flavins, as well as indolic metabolites [10,14,15,17].

5. Conclusions

Fluorescence spectroscopy of urine samples from cats diagnosed with renal and urinary disorders revealed distinct variations in emission spectra, correlated with the nature and severity of the pathological process. Emission maxima between 390–450 nm are attributed to aromatic fluorophores, derivatives of tryptophan, whereas emission bands between 500–620 nm are associated with flavin compounds, bile pigments, and oxidation products. The presence of emission bands around 390 nm represents a potential spectral marker for bacterial urinary tract infections, due to specific indoxyl compounds. Spectrofluorimetric analysis of feline urine allows the identification of biochemical changes specific to renal disorders by examining intensity variations in the emission bands characteristic of tryptophan metabolites. The results indicate a decrease in fluorescence intensity at λ_ex = 280 nm and an increase at λ_ex = 400 nm in cats with urinary infections and renal impairment, confirming the potential of this method as a rapid, non-invasive, and sensitive tool for etiological diagnosis. This method proves to be a valuable instrument in veterinary metabolomic studies, providing rapid and non-invasive insights into kidney functional status. In future research, integrating fluorescence spectroscopy with chromatographic methods and multivariate statistical analysis could enable the identification of specific biomarkers for the early diagnosis of renal diseases in cats.

The study is limited by the small number of cases, the heterogeneity of the included conditions, the single time-point evaluation, and the variability of urine collection methods, factors that may affect the robustness and generalizability of the results.

Author Contributions: Conceptualization, M.T. and I.P.; methodology, R.L.; software, C.N.; validation, I.P.; formal analysis, C.N.; investigation, A.R.; resources, A.R.; data curation, C.N.; writing-original draft preparation, M.T.; writing-review and editing, M.T.; visualization, C.N.; supervision, I.P.; project administration, I.P.; funding acquisition, R.L. All authors have read and agreed to the published version of the manuscript.

Funding: This research received no external funding

Institutional Review Board Statement: Not applicable.

Conflicts of Interest: The authors declare no conflict of interest.

References

1. Khreisha R., Haddad N. A review on non-invasive renal function assessment technologies. *J Cardiovasc Dis Res* **2021**, *12(4)*. doi.org/10.31838/jcdr.2021.12.04.07
2. Domínguez M., García-Fernández A., Martí-Centelles V., Sancenón F., Blandez J.F., Martínez-Máñez R. Renal-clearable probes for disease detection and monitoring. *Trends Biotechnol* **2025**, *43(6)*, 1286–1301. doi.org/10.1016/j.tibtech.2024.11.020
3. Madhuri, S., N. Vengadesan, P. Aruna, D. Koteeswaran, P. Venkatesan, S. Ganesan. Native fluorescence spectroscopy of blood plasma in the characterization of oral malignancy. *Photochem Photobiol* **2003**, *78(2)*, 197-202. doi:10.1562/0031-8655(2003)078<0197: nfsobp>2.0.co;2.
4. Perinchery S.M., Kuzhiumparambil U., Vemulpad S., Goldys E.M. The potential of autofluorescence spectroscopy to detect human urinary tract infection, *Talanta* **2010**, *82(3)*, 912–917. doi:10.1016/j.talanta.2010.05.049.
5. Saude, E. J., D. Adamko, B. H. Rowe, T. Marrie, B. D. Sykes, Variation of metabolites in normal human urine. *Metabolomics* **2007**, *3*, 439–451. doi:10.1007/s11306-007-0091-1.
6. Anwer A.G., Sandeep P.M., Goldys E.M., Vemulpad S. Distinctive autofluorescence of urine samples from individuals with bacteriuria compared with normals. *Clin Chim Acta* **2009**, *401(1-2)*, 73-5. doi:10.1016/j.cca.2008.11.021.
7. Geddes C.D., Lakowicz J.R. Reviews in Fluorescence, 2006, 1st ed, Springer US. Boston, MA. ISBN 978-0-387-29342-4.
8. Monici, M. Cell and tissue autofluorescence research and diagnostic applications. *Biotechnol Annu Rev*, Elsevier, **2005**, *11*, 227–256.
9. Ramanujam N. Fluorescence Spectroscopy In *Vivo, Encyclopedia of Analytical Chemistry*, *Ed. John Wiley & Sons Ltd, Chichester*, **2006**, pp. 20-56. ISBN 978-0-470-02731-8.
10. Lakowicz, J.R. Principles of Fluorescence Spectroscopy, 3rd ed.; *Springer*, 2006.
11. Leiner M.J.P., Hubmann M.R., Wolfbeis O.S. The total fluorescence of human urine. *Anal Chim Acta* **1987**, *198*, 13–23. doi.org/10.1016/S0003-2670(00)85002-3.
12. Hamdan M. Fluorescence spectroscopy applications in metabolomics and biomarker discovery. *J Fluoresc*, **2007**, *17(3)*, 401–413. doi: 10.1007/s10895-007-0214-2
13. Kušnír J., Dubayová Katarína, Lešková Lucia, Lajtár M. Fluorescence analysis of human urine: diagnostic potential and spectral features. *J Photochem Photobiol B, Biol.* **2005**, **79(1)**, 1–9. doi: 10.1016/j.jphotobiol.2004.10.007
14. Anwer A.G. Fluorescence spectroscopy of urinary biomarkers related to tryptophan metabolism. *Anal Bioanal Chem* **2009**, *393(6–7)*, 1553–1561. doi: 10.1007/s00216-008-2483-8
15. Wang I.K., Ho D.R., Chang H.Y., Lin C.L., Chuang F.R. Purple urine bag syndrome in a hemodialysis patient. *Internal Med* **2005**, *44*, 859–61. doi.10.2169/internalmedicine.44.859.
16. Bar K. Spectroscopic detection of indolic compounds in biological fluids as biomarkers of infection. *Biospectroscopy* **2007**, 13(4), *245–252*. doi: 10.1002/bio.1023
17. Bar-Or D., Rael L.T., Bar-Or R., Craun M.L., Statz J, Garrett R.E. Mass spectrometry analysis of urine and catheter of a patient with purple urinary bag syndrome. *Clin Chim Acta* **2007**, *378*, 216–8. doi.10.1016/j.cca.2006.11.015.

CVJ CLUJ VETERINARY JOURNAL

Research article

Impact of early phytobiotic and prebiotic supplementation on growth performance trajectories in broiler chickens: a time × treatment interaction study

Cîmpean Adrian [1*], Pojar Tudor Nicolae [1], Giulia Mariș [1], Ilie Antal [1], Borzan Mihai Marian [1]

[1] Department of Animal breeding and Animal Productions, University of Agricultural Science and Veterinary Medicine, Faculty of Veterinary Medicine Cluj-Napoca, Romania, adrian.cimpean@usamvcluj.ro
* Correspondence: adrian.cimpean@usamvcluj.ro

Abstract: This study evaluated the effects of early dietary supplementation with phytobiotic (nettle flour) and phytobiotic–prebiotic (alfalfa flour) additives on the growth performance of Ross 308 broiler chickens. A total of 90 one-day-old chicks were allocated to three dietary treatment groups (control, nettle, and alfalfa), each consisting of 30 birds in three replicates of 10 birds. Feed additives were administered during the first 7 days post-hatch, followed by a common basal diet across all groups until day 35. Body weight was recorded on days 7, 21, and 35. Statistical analyses included one-way ANOVA, two-way ANOVA with interaction, Ordinary Least Squares (OLS) regression, and Welch's ANOVA to account for heteroscedasticity and non-normal distributions. Significant treatment effects were observed at all time points, with a marked divergence emerging by day 35 ($F(2, 87) = 138.78$, $p < 0.0001$). Post-hoc analyses confirmed that nettle flour led to the greatest increase in body weight compared to both the control and alfalfa groups ($p < 0.001$). The alfalfa group exhibited a moderate but statistically significant effect ($p < 0.05$). Two-way ANOVA revealed a strong treatment × time interaction ($F = 90.93$, $p < 0.0001$), indicating that the efficacy of the additives varied across developmental stages. OLS regression confirmed the robustness of the model ($R^2 = 0.957$), with the "Nettle × Day 35" interaction contributing an estimated +715 g gain in body weight over the control. These findings highlight the potential of short-term early phytobiotic and prebiotic supplementation to produce long-term enhancements in broiler growth performance. Nettle flour, in particular, demonstrated superior efficacy, suggesting its potential as a functional feed additive in intensive poultry systems.

Keywords: broiler chickens; phytobiotics; prebiotics; early-life nutrition; growth performance

Received: 11.09.2025
Accepted: 01.10.2025
Published: 05.03.2026

DOI:10.52331/v31i13975

1. Introduction

The increasing global demand for poultry meat has accelerated the development of intensive broiler production systems. Within these systems, maximizing growth performance while maintaining animal health and minimizing the use of synthetic growth promoters is a core challenge. Traditional reliance on antibiotic growth promoters has diminished due to regulatory restrictions and public health concerns, prompting the search for effective and sustainable nutritional alternatives [3].

Among the most promising candidates are phytobiotics and prebiotics, which are increasingly used in poultry nutrition to improve growth rates, feed efficiency, and gut health [5,6]. Phytobiotics—bioactive compounds derived from plants—are known to exhibit antioxidant, anti-inflammatory, and antimicrobial properties [1,5]. These effects can support the immune system, enhance nutrient absorption, and promote gastrointestinal stability in broilers [4,5]. Prebiotics, defined as non-digestible dietary components that selectively stimulate the growth of beneficial intestinal bacteria, can further modulate the gut microbiota and contribute to improved feed conversion and growth performance [2,7].

Despite extensive research on these compounds, most studies focus on their continuous inclusion in the diet throughout the entire production cycle. However, the early post-hatch period represents a critical window in broiler development, during which the

digestive and immune systems undergo rapid maturation [8]. Short-term nutritional interventions during this phase may have long-lasting effects on growth performance due to developmental programming mechanisms [8]. The concept of early-life feed additive application—particularly during the first week—has therefore gained increasing interest for its potential to trigger positive physiological trajectories.

Additionally, many nutritional studies in poultry apply statistical methods that examine treatment effects at isolated time points, without considering potential interaction effects between treatment and time. Such an approach may overlook the dynamic and cumulative nature of dietary interventions. Incorporating a time × treatment interaction analysis can provide a more comprehensive understanding of how the timing and duration of supplementation influence growth outcomes [9].

The present study aimed to evaluate the effects of early dietary supplementation (during the first 7 days of life) with phytobiotic (nettle flour) and phytobiotic–prebiotic (alfalfa flour) feed additives on the growth performance trajectory of Ross 308 broiler chickens. Nettle (Urtica dioica) has been previously investigated as a natural phytogenic additive capable of improving productive performance and meat quality in broilers [10]. Body weight was monitored on days 7, 21, and 35 to assess both immediate and long-term impacts of the interventions. In addition to conventional statistical analyses, advanced modeling techniques—including two-way ANOVA with interaction terms and regression modeling—were used to detect time-dependent effects and quantify their magnitude.

It was hypothesized that short-term inclusion of plant-based feed additives in the early post-hatch period would result in significant and sustained improvements in growth performance, with measurable interaction effects depending on treatment type and developmental stage.

2. Materials and Methods

The experiment was conducted over a 35-day period on Ross 308 broiler chickens, maintained under controlled environmental conditions. Ninety one-day-old chicks were randomly assigned to three dietary treatment groups, each consisting of 30 birds divided into three replicates of 10 birds per pen. The experimental layout followed a completely randomized design to ensure unbiased allocation.

Chicks were housed in deep-litter floor pens within a temperature- and humidity-controlled facility. They had unrestricted access to feed and water throughout the trial. Environmental parameters—including temperature, humidity, and ventilation—were continuously monitored and adjusted according to the Ross 308 commercial management guidelines. Lighting was set to 23 hours light and 1 hour darkness during the first week and was later adjusted to 18 hours light and 6 hours darkness from day 8 until the end of the study.

All diets were formulated to meet or exceed the nutritional recommendations of the NRC (1994) for broiler chickens. Three dietary treatments were tested. The control group received a standard basal diet with no additives. A second group received the same basal diet supplemented with 0.5% nettle flour (*Urtica dioica*), and the third group received 0.5% alfalfa flour (*Medicago sativa*) added to the basal diet. These additives were included only during the first 7 days post-hatch, after which all groups were fed the same standard basal diet. Feed and water were provided ad libitum throughout the entire period.

Body weight was recorded individually on days 7, 21, and 35 using a digital scale with 1-gram precision. These time points were selected to capture the early growth response, intermediate phase development, and final body weight at market age. Birds were monitored daily for feed intake, general behavior, and signs of illness. No clinical issues or mortalities were observed during the study.

Statistical analysis was performed using Python 3.11 and relevant scientific libraries including statsmodels, scipy, and pingouin. Data were expressed as means ± standard deviation, and statistical significance was set at $p < 0.05$. One-way ANOVA was used to evaluate treatment effects at each time point, followed by Tukey's Honest Significant Difference (HSD) test for pairwise comparisons. To assess the combined influence of treatment and time, a two-way ANOVA with interaction was conducted on the full dataset. In addition, Ordinary Least Squares (OLS) regression modeling was applied to quantify the contributions of each factor and their interaction to final body weight. When the assumptions of normality and homogeneity of variances were not met, as determined by the Shapiro–Wilk and Levene's tests, Welch's ANOVA was used as a robust alternative. Graphical tools, including boxplots and interaction plots, were employed to visually support the statistical interpretations and highlight growth trends across treatments.

3. Results

Statistical Results and Scientific Interpretation — Effects of Phytobiotic Supplementation on Body Weight in Ross 308 Broiler Chickens. To assess the impact of dietary supplementation with phytobiotic (nettle flour) and phytobiotic–prebiotic (alfalfa flour) additives on growth performance, we evaluated body weight progression at three critical time points: day 7, day 21, and day 35. The data were analyzed using one-way ANOVA followed by Tukey's HSD post-hoc tests, and further validated through two-way ANOVA with interaction and linear regression modeling.

Day 7 – Early Onset of Growth Differentiation. At 7 days of age, a statistically significant effect of treatment was observed ($F(2, 87) = 4.28$, $p = 0.0168$). Post-hoc comparisons revealed a significant increase in body weight in the alfalfa group compared to the control ($p < 0.05$). The nettle group showed no significant difference from the control, although the contrast with the alfalfa group approached marginal significance ($p \approx 0.05$). These findings suggest that the alfalfa-based phytobiotic–prebiotic had an early stimulatory effect on body weight, while nettle exhibited a moderate, less pronounced response.

Day 21 – Intermediate Phase with Borderline Significance. By day 21, the differences between groups remained statistically borderline ($F(2, 87) = 3.11$, $p = 0.0498$). Tukey's test identified a marginally significant difference between the control and nettle groups, whereas comparisons involving the alfalfa group did not reach significance. These results indicate a tendency toward improved body weight in the nettle group, yet without sufficient statistical robustness to confirm a definitive effect at this stage.

Day 35 – Clear and Highly Significant Divergence. At the end of the feeding trial (day 35), treatment effects became highly significant ($F(2, 87) = 138.78$, $p < 0.0001$). All pairwise comparisons were statistically significant ($p < 0.001$), confirming a strong divergence among treatments. Chickens in the nettle group achieved the highest final body weights, significantly surpassing both the control and alfalfa groups. The alfalfa group demonstrated an intermediate effect, indicating a positive but less potent influence compared to nettle supplementation (Table 1).

Advanced Statistical Analysis — Two-Way ANOVA and Linear Regression. A two-way ANOVA with interaction was conducted to evaluate the combined effects of dietary treatment and age on broiler body weight (Fig. 1). The results confirmed highly significant main effects for both treatment ($F = 118.45$, $p = 2.48 \times 10^{-37}$) and time ($F = 2591.75$, $p = 6.74 \times 10^{-173}$), as well as a highly significant interaction between the two factors ($F = 90.93$, $p = 2.62 \times 10^{-48}$). This interaction indicates that the efficacy of dietary additives is time-dependent and varies across growth stages.

To quantify these effects, an ordinary least squares (OLS) regression model was applied, yielding an R^2 value of 0.957, suggesting that the model explained 95.7% of the total variance in body weight. Notably, the interaction term "Nettle × Day 35" emerged as a major contributor, associated with an estimated +715 g increase in body weight compared to the baseline (control at 21 days). This underscores the potent and time-amplified effect of nettle supplementation in the final phase of growth.

Dietary inclusion of plant-based feed additives—specifically, nettle flour (phytobiotic) and alfalfa flour (phytobiotic–prebiotic)—exerted a statistically significant influence on body weight in Ross 308 broiler chickens. A cumulative, time-dependent effect was evident, with the most pronounced differences occurring at day 35. Among the tested treatments, nettle flour led to the greatest weight gain, contributing an additional 715 g over the baseline. These findings demonstrate the potential of phytobiotic feed strategies as functional growth promoters in broiler production, particularly in enhancing performance during the later stages of development.

The boxplot illustrates the distribution of body weight across three dietary treatments: control (standard feed), phytobiotic (nettle flour), and phytobiotic–prebiotic (alfalfa flour) over a 35-day rearing period. At 7 days, group differences were minor; however, by day 21, a moderate increase in median weight was observed in the Nettle group. A substantial divergence appears at day 35, where Nettle flour supplementation led to a significantly higher median weight and narrower interquartile range, suggesting both enhanced growth and reduced variability. The Alfalfa group showed intermediate performance, while the control group consistently recorded the lowest weight values. These results support a time-dependent effect of phytobiotic interventions on growth performance in broilers.

The interaction plot displays the mean body weight (± SD) of Ross 308 broiler chickens subjected to three dietary treatments: control, phytobiotic (nettle flour), and phytobiotic–prebiotic (alfalfa flour), assessed at 7, 21, and 35 days of age.

Table 1. Body weight (g) of Ross 308 broiler chickens at 7, 21, and 35 days after population under dietary supplementation with phytobiotic and phytobiotic–prebiotic feed additives.

No.	Control (7 d) (*g*)	Nettle Flour (7 d) (*g*)	Alfalfa Flour (7 d) (*g*)	Control (21 d) (*g*)	Nettle Flour (21 d) (*g*)	Alfalfa Flour (21 d) (*g*)	Control (35 d) (*g*)	Nettle Flour (35 d) (*g*)	Alfalfa Flour (35 d) (*g*)
1.	288	300	368	1124	952	1094	1325	2210	1545
2.	267	263	285	1074	1102	996	1680	2682	1645
3.	315	302	276	442	1204	1070	1685	2364	1730
4.	304	284	333	1296	1196	1028	1332	2722	1400
5.	325	310	318	1080	1407	1110	1588	2534	1688
6.	290	294	287	1182	1072	1042	1560	2284	1608
7.	275	337	324	1056	1116	966	1455	2686	1760
8.	281	336	302	1302	1098	1200	1750	2324	1528
9.	226	315	273	1136	1334	1284	1636	2022	1450
10.	286	303	346	954	1132	992	1910	2146	1525
11.	222	325	310	1242	1148	890	1335	2372	1530
12.	321	334	283	1000	1264	1186	495	2010	1721
13.	306	280	352	838	1064	1112	1570	2102	1655
14.	286	317	326	1176	1188	1134	1470	2690	1705
15.	301	300	300	1190	1092	1008	1625	2520	1505
16.	198	242	332	822	1244	1166	1723	2426	1450
17.	240	292	340	1214	1296	1135	1790	2316	1620
18.	318	279	312	992	1194	1154	1575	2216	1610
19.	296	317	283	1140	1164	1096	1490	2244	1725
20.	320	284	358	1135	1155	1124	1370	2516	1700
21.	245	298	318	1076	1088	1134	1480	2084	1710
22.	281	328	334	1126	1204	1012	1610	2350	1210
23.	308	330	329	1166	1166	1172	1640	2226	1440
24.	337	275	264	1182	984	1204	1635	2454	1340
25.	296	280	235	1056	1030	1048	1605	2506	1325
26.	310	289	280	1148	1386	1169	1850	2360	1420
27.	300	292	310	1110	964	876	1825	2204	1710
28.	283	275	302	876	1050	1214	1635	2206	1740
29.	276	299	260	1102	1216	1135	1782	2140	1660
30.	290	288	312	1044	1185	1192	1555	2741	1800
Media	286.37	298.93	308.40	1076.03	1156.50	1098.10	1566.03	2355.23	1581.83

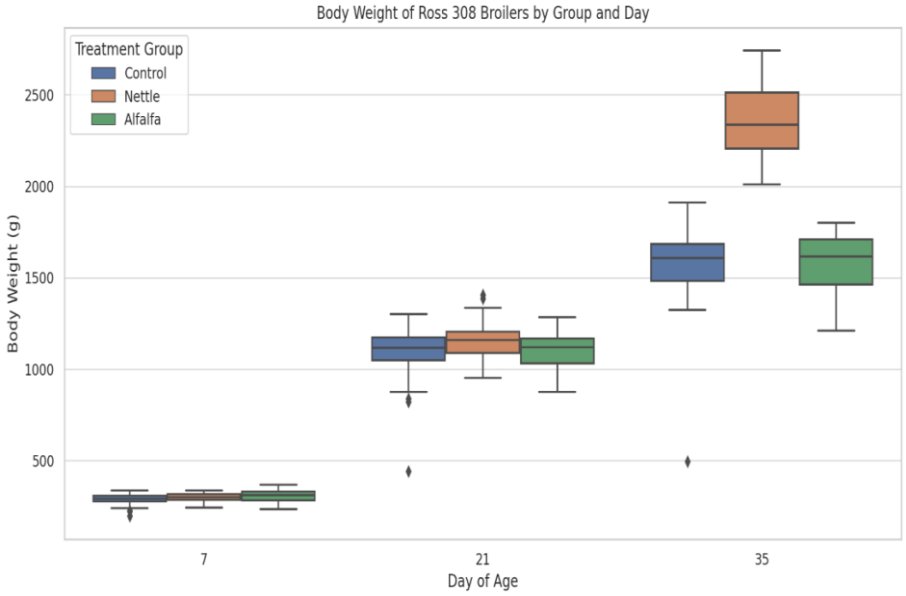

Figure 1. Distribution of body weight (g) of Ross 308 broiler chickens at 7, 21, and 35 days post-population under different dietary treatments.

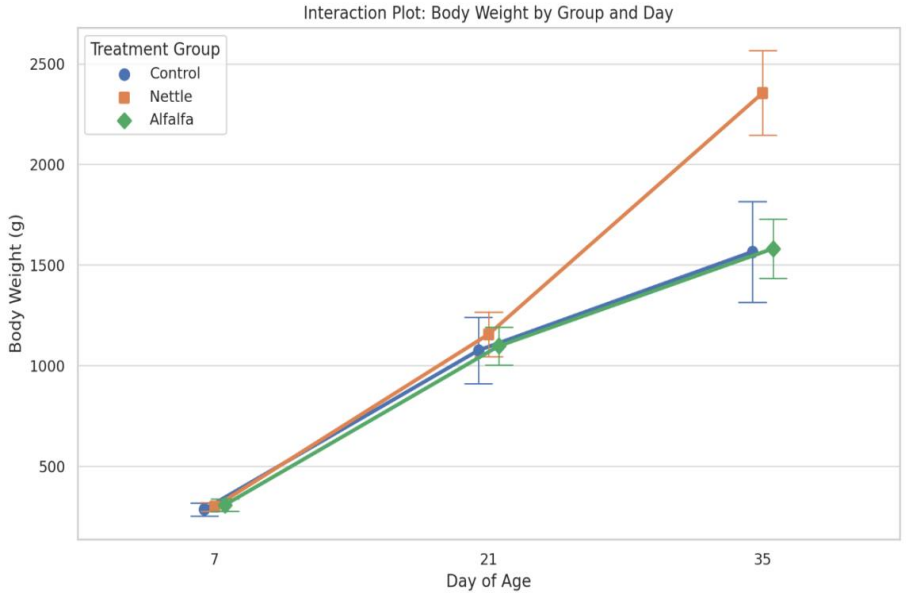

Figure 2. Interaction plot showing the effect of dietary treatment and age on the body weight of Ross 308 broiler chickens.

A marked interaction effect is evident, particularly at day 35, where the Nettle group diverges sharply, exhibiting the highest growth trajectory. The lines representing the three groups are non-parallel, indicating a significant treatment × time interaction, as supported by ANOVA ($p < 0.0001$).

General Statistical Analysis – Overall Comparison of Treatment Groups. To evaluate the overall effect of dietary supplementation on broiler growth, we conducted a one-way ANOVA on the full dataset ($n = 270$), combining data from all time points. This approach allowed us to assess the average impact of each dietary treatment—control, alfalfa (phytobiotic–prebiotic), and nettle (phytobiotic)—regardless of the age of the birds.

The analysis revealed a statistically significant effect of treatment group on body weight ($F(2, 267) = 5.45$, $p = 0.0048$), indicating that, when considered across all time points, the type of feed additive influenced growth performance. Post-hoc comparisons using Tukey's HSD test showed that both supplemented groups had higher mean body weights compared to the control group. Specifically, the alfalfa group exhibited a moderate but statistically significant increase ($p = 0.045$), while the nettle group showed a more pronounced

effect ($p = 0.001$). Although the nettle group also outperformed the alfalfa group in terms of mean body weight, this difference did not reach statistical significance ($p = 0.097$) (Fig. 2).

These findings suggest that both phytobiotic and phytobiotic–prebiotic supplementation support enhanced growth in broiler chickens, with nettle flour appearing to have a stronger effect overall.

To verify the validity of the ANOVA results, we tested the underlying assumptions of normality and homogeneity of variances. The Shapiro–Wilk test revealed significant deviations from normality in all three groups ($p < 0.05$), indicating that body weight data were not normally distributed. Additionally, Levene's test for homogeneity of variances also failed ($p < 0.001$), showing that the variability in body weight differed significantly between groups.

Given these violations of ANOVA assumptions, we applied Welch's ANOVA—a robust alternative that does not assume equal variances. The results remained statistically significant ($F(2, 172.68) = 4.09$, $p = 0.0183$), confirming the presence of treatment effects on body weight. Mean values across all time points further supported this conclusion: chickens in the nettle group had the highest average body weight (1270.2 g), followed by alfalfa (996.1 g), and control (976.1 g).

In summary, the statistical evidence consistently indicates that dietary supplementation, particularly with nettle flour, contributes to improved growth performance in Ross 308 broilers. These effects persist even when model assumptions are violated, reinforcing the reliability of the observed treatment differences.

While early-stage differences (day 7) are minimal, the later-stage divergence highlights the time-dependent synergistic effect of the phytobiotic intervention, particularly in the Nettle group.

4. Discussion

The increasing global demand for poultry meat has accelerated the development of intensive broiler production systems. Within these systems, maximizing growth performance while maintaining animal health and minimizing the use of synthetic growth promoters is a core challenge. Traditional reliance on antibiotic growth promoters has diminished due to regulatory restrictions and public health concerns, prompting the search for effective and sustainable nutritional alternatives [3].

Among the most promising candidates are phytobiotics and prebiotics, which are increasingly used in poultry nutrition to improve growth rates, feed efficiency, and gut health [5,6]. Phytobiotics—bioactive compounds derived from plants—are known to exhibit antioxidant, anti-inflammatory, and antimicrobial properties [1,5]. These effects can support the immune system, enhance nutrient absorption, and promote gastrointestinal stability in broilers [4,5]. Prebiotics, defined as non-digestible dietary components that selectively stimulate the growth of beneficial intestinal bacteria, can further modulate the gut microbiota and contribute to improved feed conversion and growth performance [2,7].

Despite extensive research on these compounds, most studies focus on their continuous inclusion in the diet throughout the entire production cycle. However, the early post-hatch period represents a critical window in broiler development, during which the digestive and immune systems undergo rapid maturation [8]. Short-term nutritional interventions during this phase may have long-lasting effects on growth performance due to developmental programming mechanisms [8]. The concept of early-life feed additive application—particularly during the first week—has therefore gained increasing interest for its potential to trigger positive physiological trajectories.

Additionally, many nutritional studies in poultry apply statistical methods that examine treatment effects at isolated time points, without considering potential interaction effects between treatment and time. Such an approach may overlook the dynamic and cumulative nature of dietary interventions. Incorporating a time × treatment interaction analysis can provide a more comprehensive understanding of how the timing and duration of supplementation influence growth outcomes [9].

The present study aimed to evaluate the effects of early dietary supplementation (during the first 7 days of life) with phytobiotic (nettle flour) and phytobiotic–prebiotic (alfalfa flour) feed additives on the growth performance trajectory of Ross 308 broiler chickens. Nettle (Urtica dioica) has previously been reported as a plant-based additive capable of improving productive performance and meat quality in broilers [10]. Body weight was monitored on days 7, 21, and 35 to assess both immediate and long-term impacts of the interventions. In addition to conventional statistical analyses, advanced modeling techniques—including two-way ANOVA with interaction terms and regression modeling—were used to detect time-dependent effects and quantify their magnitude.

It was hypothesized that short-term inclusion of plant-based feed additives in the early post-hatch period would result in significant and sustained improvements in growth performance, with measurable interaction effects depending on treatment type and developmental stage.

5. Conclusions

This study demonstrates that early-life supplementation with plant-derived feed additives—specifically nettle flour (phytobiotic) and alfalfa flour (phytobiotic–prebiotic)—can exert significant, time-dependent effects on growth performance in Ross 308 broiler chickens.

Although the additives were included only during the first 7 days post-hatch, their influence persisted and intensified over time, culminating in significant body weight differences at day 35. Among the tested treatments, nettle flour produced the highest final body weight (2355.2 g), exceeding both the control (1566.0 g) and alfalfa (1581.8 g) groups ($p < 0.001$). The early administration of nettle was associated with a +715 g weight gain, as quantified by OLS regression modeling, underscoring its long-term anabolic effect.

While alfalfa flour induced a moderate improvement in early growth (day 7), its effect diminished by day 21 and did not translate into a significant long-term gain. This suggests a transient prebiotic effect, less effective than the more persistent action observed in the nettle group.

The statistical robustness of these findings was confirmed through two-way ANOVA, Welch's ANOVA, and regression modeling, revealing a strong treatment × time interaction and validating the efficacy of early phytobiotic interventions.

In conclusion, short-term phytobiotic supplementation during the early post-hatch period may represent a viable strategy to enhance broiler productivity without continuous additive use. Nettle flour, in particular, emerges as a promising candidate for improving final body weight in intensive poultry systems, supporting its potential integration into functional feed programs aimed at optimizing performance while reducing reliance on synthetic growth promoters.

Author Contributions: Conceptualization, C. A. and P. T. N.; Methodology, C. A. and P. T. N.; Validation, C. A., P. T. N. and B. M. M.; Data Analysis, C.A.; Investigation, C. A. and P. T. N.; Resources, P.T.N.; Writing – Original Draft Preparation, C.A.; Writing – Review & Editing, P.T.N. and B.M.M.; Visualization, C.A.; Supervision, P.T.N.; Project Administration, P.T.N. All authors have read and agreed to the published version of the manuscript.

Funding: This research received no external funding.

Institutional Review Board Statement: Not applicable.

Data Availability Statement: The original contributions presented in this study are included in the article. Further inquiries can be directed to the corresponding author.

Acknowledgments: This research was supported by the University of Agricultural Sciences and Veterinary Medicine Cluj-Napoca.

Conflicts of Interest: The author declares no conflict of interest.

References

1. Khatun, A.; Das, S.C.; Ray, B.C.; Ahmed, T.; Hashem, M.A.; Khairunnesa, M.; Roy, B.C. Effects of feeding phytobiotics on growth performance, breast meat quality, blood biochemical indices, and liver enzymes of broiler chickens. *Europ Poult Sci* **2023**, *87*: Article 374.
2. Naeem, M., Bourassa, D. Probiotics in poultry: Unlocking productivity through microbiome modulation and gut health. *Microorganisms* **2025**, *13(2)*, 257.
3. Wickramasuriya, S. S., Ault, J., Ritchie, S., Gay, C. G., Lillehoj, H. S. Alternatives to antibiotic growth promoters for poultry: A bibliometric analysis of the research journals. *Poult Sci* **2024** *103(9)*, 103987.
4. Peng, H., Zhang, L., Zhao, L., Xing, T., Gao, F. Benzoic acid and oregano essential oil interact to increase the immune function and intestinal development of Langshan chickens. *Br Poult Sci* **2026,** 1-12.
5. Obianwuna, U. E., Chang, X., Oleforuh-Okoleh, V. U., Onu, P. N., Zhang, H., Qiu, K., Wu, S. Phytobiotics in poultry: Revolutionizing broiler chicken nutrition with plant-derived gut health enhancers. *J Anim Sci Biotechnol*, **2024**, *15*, 169.
6. Abd El-Ghany, W. Phytobiotics in poultry industry as growth promoters, antimicrobials and immunomodulators: A review. *J World's Poult Res* **2020**, *10(4)*, 571–579.
7. Patterson, J. A., Burkholder, K. M. Application of prebiotics and probiotics in poultry production. *Poult Sci* **2003**, *82(4)*, 627–631.
8. Gaweł, A., Madej, J. P., Kozak, B., Bobrek, K. Early post-hatch nutrition influences performance and muscle growth in broiler chickens. *Animals* **2022**, *12(23)*, 3281.

9. Marx, F. O., Alvarez, M. V. N., Bassi, L. S., Félix, A. P., Krabbe, E. L., Oliveira, S. G., Maiorka, A. Use of statistical models to determine the optimal concentration of metabolizable energy for growth performance of broiler chickens. *Livest Sci* **2023**, *274*, 105268.
10. Mierlița, D., Davidescu, M. A., Doliș, M. G., Simeanu, D., Pop, I. M. The effect of nettle flour (Urtica dioica) in diets for broiler chickens on productive performance, lipid quality and oxidative stability of meat. *Ann Univ Oradea*, **2023**, Fascicle: Ecotoxicology, Animal Science and Food Science and Technology.

CVJ CLUJ VETERINARY JOURNAL

Review article

Emerging Biomarkers in Canine Glaucoma: Insights into Clinical, Genetic, Oxidative, and Inflammatory Pathways

Luh Made Nanda Ayuni [1], Ida Tjahajati [2], Ida Fitriana [3,*]

[1] Magister Sain Veteriner, Faculty of Veterinary Medicine, Universitas Gadjah Mada, Yogyakarta, Indonesia
[2] Department of Internal Medicine, Faculty of Veterinary Medicine, Universitas Gadjah Mada, Yogyakarta, Indonesia
[3] Department of Pharmacology, Faculty of Veterinary Medicine, Universitas Gadjah Mada, Yogyakarta, Indonesia
* Correspondence: ida.fitriana@ugm.ac.id

Abstract: Canine glaucoma is a complex ocular disorder characterized by the progressive loss of retinal ganglion cells (RGCs) and specific optic nerve damage, often resulting in permanent blindness in affected dogs. Recent advancements highlight the importance of various biomarkers in understanding the development and progression of canine glaucoma, particularly in relation to clinical signs, genetics, oxidative stress, and inflammatory pathways. An imbalance between aqueous humor production and drainage significantly affects intraocular pressure (IOP), a key factor in managing glaucoma. Oxidative stress has emerged as a key contributor to RGC degeneration in canine glaucoma, mirroring findings in human studies, where it is implicated in glaucomatous neurodegeneration. The interaction between oxidative stress and pro-inflammatory cytokines such as tumor necrosis factor-alpha (TNF-α) in the aqueous humor reflects a complex biomarker network with potential diagnostic and therapeutic value. The identification of genetic biomarkers, including enzyme and protein variants, also indicates a move toward molecular methods for evaluating glaucoma risk across different dog breeds. Understanding these interconnected factors offers valuable insights into novel treatments and preventive measures, including genetic screening, oxidative stress monitoring, anti-inflammatory and neuroprotective therapies. Continued biomarker research is essential for improving clinical outcomes in canine glaucoma and may also offer translational relevance to human glaucomatous diseases, thereby broadening future therapeutic possibilities.

Keywords: canine glaucoma; clinical biomarker; genetic biomarker; inflammation biomarker; oxidative stress biomarker.

1. Introduction

Canine glaucoma is a complex eye condition mainly marked by increased intraocular pressure (IOP), which leads to the gradual loss of retinal ganglion cells (RGCs) and vision problems [1]. Glaucoma has become a leading cause of blindness in dogs, highlighting the need for better understanding and treatment of the disease. The prevalence of canine glaucoma varies across studies and populations. A study conducted at the University of Zurich between 1995 and 2009 found that secondary glaucoma accounted for only 3.6% of all new canine ophthalmology cases examined, highlighting its relative rarity within that specific population. In contrast, another study from California reported a higher prevalence of 6.9% for secondary glaucoma cases [2]. Such discrepancies may be attributed to differences in geographic or clinical settings and the effectiveness of managing underlying conditions that predispose dogs to secondary glaucoma. Diagnosing and managing canine glaucoma heavily depends on finding biomarkers, essential signs of the disease, and its progression [3].

Glaucoma is particularly common in certain dog breeds, and studies show that genetic factors play a role in its occurrence [4]. Clinical biomarkers like IOP, retinal nerve fiber layer (RNFL) thickness, and changes in the optic nerve head (ONH) are key to assessing damage caused by glaucoma. Advanced tools such as optical coherence tomography (OCT) enable accurate measurement of the RNFL, helping with early detection and monitoring of the disease. Precise measurement of IOP and careful examination of

Received: 31.07.2025
Accepted: 13.10.2025
Published: 05.03.2026

DOI:10.52331/V31i1dz34

the ONH are also central to understanding the structural changes linked to glaucoma [5]. Beyond clinical tests, research into genetic biomarkers has become more critical in veterinary eye care. Specific gene mutations, such as those in the myocilin gene, are associated with primary open-angle glaucoma across different breeds. Understanding these genetic factors not only helps identify vulnerable populations but also opens the door to gene therapy treatments [6].

Oxidative stress is increasingly seen as a key part of how glaucoma develops. Higher levels of oxidative stress markers, such as malondialdehyde (MDA), show cellular damage within the retina and contribute to RGC death. The relationship between oxidative stress and high IOP suggests that therapies aimed at reducing oxidative damage could protect retinal tissue and help maintain vision in affected dogs [7]. Inflammation is recognized as a significant factor in glaucoma progression. Increased levels of pro-inflammatory cytokines, such as tumor necrosis factor-alpha (TNF-α), are found in glaucomatous eyes and further damage the retina [8].

The complex nature of canine glaucoma calls for a comprehensive approach that includes clinical, genetic, oxidative stress, and inflammatory biomarkers [9]. These insights could improve diagnosis and treatment efforts to prevent vision loss from this severe disease. A better understanding of these biomarkers can lead to more effective management and tailored therapies, ultimately preserving sight and enhancing quality of life for affected dogs. This all-encompassing strategy aims to improve diagnostics and develop better treatments to improve outcomes in veterinary ophthalmology.

2. Results and Discussion

2.1 Pathophysiology

The pathogenesis of glaucoma in canines, as in humans, is a multifactorial process characterized primarily by the progressive degeneration of RGCs and their axons, often triggered by elevated IOP. Canine glaucoma can be classified as primary open-angle glaucoma (POAG) and primary angle-closure glaucoma (PACG), each exhibiting differences in clinical manifestations and underlying structural changes [10]. A significant aspect of canine primary glaucoma is its genetic component; certain breeds show a higher predisposition to this disease due to hereditary factors. For example, Beagles are recognized as a breed with documented anatomical predispositions related to glaucoma [5]. Such genetic factors can result in anatomical anomalies affecting the iridocorneal angle, facilitating the onset of elevated IOP and playing a crucial role in understanding the disease's pathophysiology [11].

Inflammation is another fundamental element contributing to the pathophysiology of canine glaucoma. Elevated levels of inflammatory cytokines, particularly interleukin-1β, have been correlated with an increased risk and progression of the disease [12]. Compromised vascular integrity in the uvea, a consequence of elevated IOP, can worsen the inflammatory response, potentially creating a pathological feedback loop that may hasten RGC degeneration [8]. Additionally, inflammation can affect medication compliance in affected dogs, as local adverse reactions to treatments can lead to discontinuation of necessary medications, further complicating management strategies [13]. Oxidative stress also plays a critical role in the etiology of glaucoma. Increased oxidative stress has been linked to excitotoxic damage of RGCs and is associated with elevated levels of glutamate and nitric oxide (NO), both of which predispose RGCs to degeneration [7]. The pathogenic effects of oxidative stress include mitochondrial dysfunction, which may impair energy metabolism in retinal cells, contributing to cumulative damage within the ocular microenvironment [14].

2.2. Clinical Biomarkers

Canine glaucoma is a complex ocular condition characterized by elevated IOP that negatively affects RGCs and the ONH. This progressive condition can result in severe vision impairment and blindness due to increased IOP and subsequent damage to the optic nerve and retinal structures [1].

2.2.1. Intraocular pressure (IOP)

Elevated IOP indicates a significant disruption of the homeostatic balance of aqueous humor dynamics, typically due to obstruction of drainage through the trabecular meshwork. Normally, IOP in dogs ranges between 10 to 25 mmHg, with elevations suggesting potential glaucomatous conditions [15]. The balance between aqueous humor production mainly regulates IOP in the ciliary body and its outflow through the trabecular meshwork and uveoscleral pathways [16]. Glaucoma occurs when there is an obstruction or functional impairment in these outflow pathways, leading to increased IOP, which can then cause optic nerve damage and vision loss [5].

The pathological mechanisms underlying glaucoma in canines encompass both mechanical and biochemical components. Elevated IOP induces stress within the ONH, characterised by deformation and potential ischaemia due to compromised blood flow [10]. Chronic IOP elevation can alter neuroretinal structures, leading to the gradual degeneration of RGCs. Specific biochemical pathways, such as excitotoxicity arising from neurotransmitter imbalances or neurotrophin deprivation, have been implicated in RGC death, independent of IOP levels [4]. This suggests that while IOP is a significant risk factor, other concurrent mechanisms also contribute to the overall pathology of canine glaucoma.

- RGCs

RGCs serve as crucial clinical biomarkers for canine glaucoma, primarily because they transmit visual information from the retina to the brain and are susceptible to elevated IOP. In canine glaucoma, similar to the human condition, elevated intraocular pressure is a significant risk factor that initiates a cascade of events, ultimately compromising retinal ganglion cell survival [3]. Due to their pivotal role in transmitting visual information, retinal ganglion cells have emerged as prime candidates for biomarker development. Monitoring RGC health and function could provide invaluable insights into glaucoma pathogenesis and facilitate the evaluation of novel therapeutic strategies. The progressive degeneration of retinal ganglion cells and the loss of their axons are characteristic of glaucoma [17].

The RGCs are a crucial link between the retina and the brain, relaying visual information essential for sight; their deterioration is a hallmark of glaucoma. This degeneration often appears as thinning of the RNFL, which correlates with the loss of RGC axons. The RNFL thinning can precede RGC soma loss, suggesting that RNFL thickness monitoring can serve as an early marker of glaucoma progression. Additionally, quantitative assessments such as OCT offer methods to evaluate structural changes in the retina that reflect RGC status [18].

- ONH

The ONH plays a critical role in understanding glaucoma pathophysiology in canines, primarily through its relationship with IOP and RGC health. In dogs, glaucomatous changes at the ONH can manifest as alterations in its appearance, reflecting possible functional deficiencies earlier than conventional visual assessments can detect [1]. Normal conditions at the ONH include a defined optic disc morphology, typical blood supply, and integrity of the nerve fibre layers. However, in glaucomatous conditions, mechanical stress from elevated IOP causes optic nerve degeneration, leading to changes in the ONH, such as cupping, increased disc pallor, and changes in shape due to nerve fibre loss. Histopathological studies have shown that ongoing inflammation, characterised by the infiltration of neutrophils and the presence of elevated pro-inflammatory cytokines like TNF-α, can correlate with changes in ocular structures and may exacerbate degenerative processes in glaucomatous eyes [13].

Abnormal conditions at the ONH in glaucomatous dogs may result from the breakdown of the blood-retinal barrier and subsequent inflammation. This inflammation can arise from increased IOP, which mechanically disrupts normal tissue architecture, and immune-mediated processes that further exacerbate damage. Such mechanisms highlight the significance of ONH assessment, as early identification of changes can influence the clinical management of canine glaucoma [19].

2.3. Genetic Biomarkers

Given its heritable nature across breeds, canine glaucoma, which is primarily genetic, presents an intriguing field of study. Emerging evidence indicates several genetic biomarkers that can aid in understanding the underlying mechanisms contributing to this ocular condition [6].

- ADAMTS10

ADAMTS10 is part of a family of metalloproteinases crucial in remodeling the extracellular matrix (ECM) in ocular tissues. Mutations in the ADAMTS10 gene have been implicated in primary glaucoma in certain breeds, such as the Basset Hound. These mutations can impair ECM turnover, disrupting normal ocular structure and function. As a result, alterations in the trabecular meshwork can hinder aqueous humor drainage, raising IOP and ultimately contributing to optic nerve damage [5].

- ADAMTS17

Like ADAMTS10, the ADAMTS17 gene encodes a protein involved in ECM remodeling. Genetic variations in ADAMTS17 have been linked to hereditary glaucoma, particularly in breeds such as the Petit Basset Griffon Vendéen (PBGV). The dysfunction arising from ADAMTS17 mutations leads to structural changes

in the eye, which can increase IOP by obstructing aqueous humor outflow pathways. This not only increases the risk of developing glaucoma but also instigates progressive optic nerve damage [11]. The MYOC gene is perhaps the best-known genetic marker for glaucoma, as it has been extensively studied in both canines and humans. The MYOC gene has been extensively studied in breeds like the *Beagle* and *Labrador Retriever*. Mutations in MYOC disrupt normal protein folding and function, leading to the accumulation of abnormal myocilin protein in the trabecular meshwork and increased resistance to aqueous humor outflow. This condition raises IOP and promotes the death of RGCs, leading to irreversible optic nerve damage typical of glaucomatous conditions [4].

- COL12A

The COL12A gene encodes collagen type XII, a critical component of the ocular ECM, and has been linked to glaucoma in breeds such as the *Shih Tzu.* Mutations in this gene can lead to weaknesses in the collagen fibers that provide structural support to the eye. This abnormality may disrupt the normal biomechanics of the eye, leading to elevated IOP through impaired drainage and contributing to glaucoma development. Abnormal collagen organization has been associated with increased resistance in aqueous humor outflow, further compounding the IOP changes that induce optic nerve damage [20].

- RAB22A

RAB22A plays a significant role in intracellular trafficking, influencing vesicle transport in ocular tissues that are associated with an increased risk of glaucoma in breeds such as the *Staffordshire Bull Terrier*. Dysregulation of this gene can lead to abnormal cellular responses in the trabecular meshwork, disrupting the normal processes of aqueous humor outflow. This disruption can lead to increased IOP as the flow of fluid through the ocular drainage system is obstructed, consequently heightening the risk of glaucomatous degeneration in the optic nerve [11].

- NEB

The NEB gene encodes nebulin, which is significant for the structural integrity of various connective tissues in breeds such as the Eurasier. Variants in NEB may alter the mechanical properties of the sclera and other ocular structures, thereby altering the eye's response to IOP fluctuations. These abnormalities can increase the susceptibility to glaucomatous changes by affecting how the ocular tissues withstand elevated pressures, ultimately leading to further optic nerve degeneration [1].

- SRBD1

The SRBD1 gene, which is associated with RNA processing, has been shown to be significantly associated with glaucoma in certain breeds, including the Shiba Inu. Specific polymorphisms in SRBD1 were associated with increased susceptibility to the disease. This gene's involvement suggests a genetic mechanism where metabolic or regulatory dysfunctions can amplify apoptotic pathways in RGCs, facilitating progressive optic nerve damage characteristic of glaucoma [21].

2.4. Oxidative Stress Biomarkers

Oxidative stress significantly contributes to the pathogenesis of canine glaucoma, as evidenced by various biomarkers indicating oxidative damage and the stress response.

- MDA

MDA is a significant biomarker of oxidative stress that provides insight into the underlying mechanisms of canine glaucoma. Elevated levels of MDA reflect lipid peroxidation, a process in which reactive species interact with cellular membrane lipids, leading to potential damage to retinal and other ocular tissues [22]. In glaucoma, MDA serves as a crucial indicator of oxidative damage that can contribute to the disease's pathophysiology. Oxidative stress in the eye occurs when the production of reactive oxygen species (ROS) exceeds the eye's antioxidant defense mechanisms. Under normal conditions, antioxidants such as glutathione (GSH) and various enzymes help mitigate oxidative damage. However, increased IOP can induce cellular stress in conditions such as glaucoma, leading to elevated ROS levels that trigger lipid peroxidation.

MDA, a byproduct of lipid peroxidation, serves as a sensitive marker of oxidative damage in the retina and other ocular tissues [23]. The cellular environment rapidly becomes hostile when dogs develop glaucomatous conditions, often due to impaired aqueous humor drainage or elevated intraocular pressure. Elevated levels of MDA indicate significant membrane damage and contribute to further inflammation and cell death within the retina, adversely affecting RGCs, which are crucial for visual function [7]. This chain of events underscores MDA's role not only as a marker but also as a contributor to degenerative processes that

lead to vision loss. Specifically, elevated MDA levels in the aqueous humor of dogs with glaucoma may also indicate an underlying inflammatory response driven by oxidative stress, further contributing to ongoing damage to the optic nerve head and subsequent degeneration of the visual pathway. Enhanced lipid peroxidation, as evidenced by elevated MDA levels, indicates that the retina struggles to cope with oxidative stress due to diminished antioxidant defenses, ultimately leading to cellular apoptosis and vision impairment [24].

- Nitrated Tyrosines (NT)

NTs are significant markers of oxidative stress associated with various ocular diseases, including canine glaucoma. NT form when reactive nitrogen species (RNS), such as peroxynitrite ($ONOO^-$), modify tyrosine residues in proteins, leading to cellular damage. This modification has been studied as a biomarker in glaucoma due to its implications for RGC health, which are particularly susceptible to oxidative stress. In canine glaucoma, elevated IOP increases ROS and RNS production, including NO, in retinal tissues. When NO reacts with superoxide anions (O_2^-), $ONOO^-$ forms, which can subsequently lead to the nitration of tyrosine residues in proteins, resulting in NT accumulation [22]. NT indicates ongoing oxidative damage to cellular proteins, impairing their normal functions. This nitration can disrupt crucial cellular signaling pathways, leading to protein misfolding or dysfunction and ultimately promoting apoptosis in RGCs. Since RGCs are integral to the transmission of visual information, their degeneration significantly contributes to vision loss in dogs affected by glaucoma [25].

- GSH

GSH is a tripeptide made up of glutamine, cysteine, and glycine, and it exists in high concentrations in retinal tissues. Its primary role is as a cellular antioxidant, neutralizing free radicals and ROS produced during metabolic processes and environmental stressors. In canine glaucoma, GSH levels can become severely altered. Studies have shown that dogs with glaucoma often exhibit significantly reduced GSH levels, adversely affecting their ability to cope with oxidative stress [7]. This reduction indicates abnormal conditions, reflecting an overwhelmed antioxidant defense system under continuous oxidative assault. When GSH levels decline, the retina becomes increasingly vulnerable to oxidative stress, which can lead to RGC degeneration. The decrease in GSH levels is associated with elevated markers of oxidative damage. Compromised GSH levels and their subsequent inability to neutralize excess ROS can lead to cellular apoptosis. This cellular stress is known to drive RGC death, further worsening the visual impairment associated with glaucoma [25].

- Advanced Glycation End-products (AGEs)

AGEs form through non-enzymatic glycation. In this reaction, reducing sugars react with proteins, lipids, or nucleic acids, resulting in structural and functional alterations in these macromolecules. In canines suffering from glaucoma, oxidative stress intensifies due to elevated IOP and subsequent tissue damage in the eye. This mechanism involves excessive ROS production, which can enhance the formation of AGEs through glycation. Elevated levels of AGEs in the aqueous humor and ocular tissues correlate with oxidative stress markers, indicating significant oxidative damage within the eye. The accumulation of AGEs can worsen oxidative stress, creating a feedback loop that further promotes degeneration of RGCs and aggravates glaucoma [8]. Glycation-induced modifications of proteins impair their function, including those essential for maintaining ocular pressure and aqueous humor dynamics. This impairment can lead to chronic elevation of IOP, further deteriorating glaucoma conditions. The AGEs have promoted apoptosis among RGCs. The binding of AGEs to RAGE activates signaling pathways that can lead to neuroinflammation and cell death. Such effects contribute to the progressive loss of vision observed in dogs with glaucoma, underscoring the importance of AGEs in the disease's progression [14].

- Total Antioxidant Capacity (TAC)

TAC is a critical biomarker of oxidative stress and is particularly significant in canine glaucoma. TAC reflects the overall ability of the eye's tissues, including the retina and aqueous humor, to counteract oxidative damage from ROS. The TAC represents the combined effects of various antioxidants in the ocular environment, including enzymes (such as superoxide dismutase, catalase, and glutathione peroxidase (GPX)) and non-enzymatic antioxidants (such as ascorbic acid and alpha-tocopherol). A delicate balance exists between ROS production and antioxidant defenses in a healthy ocular environment, facilitating normal physiological function. However, under oxidative stress conditions, such as those encountered in glaucoma, antioxidant defenses may become insufficient [8]. In canine glaucoma, elevated IOP results in increased ROS production. This oxidative stress can surpass local antioxidant defenses, including TAC, leading to damage

to RGCs and other ocular structures. A reduction in TAC indicates a diminished capacity to neutralize ROS effectively [24]. A significant decline in TAC has been associated with increased oxidative damage markers, such as MDA and protein oxidation products. In glaucomatous dogs, low TAC levels indicate an inability to protect retinal cells from ROS-mediated damage, leading to cell apoptosis and neurodegeneration. Studies indicate that decreased TAC levels are connected to the progression of RGC loss in glaucomatous conditions. The compromised antioxidant defense critically limits the retina's ability to recover from oxidative damage, thereby accelerating a pathophysiological decline in visual function [21].

- Superoxide Dismutase (SOD)

SOD is a critical enzyme in the antioxidant defense system that catalyzes the dismutation of superoxide radicals (O_2^-) into hydrogen peroxide (H_2O_2) and molecular oxygen. In glaucoma, elevated IOP leads to increased ROS production, including superoxide radicals. The accumulation of these radicals is harmful to retinal cells. SOD mitigates this risk by converting superoxide into the less harmful hydrogen peroxide, which can be further detoxified by other antioxidant enzymes like catalase (CAT) and GPX [14]. Studies have shown that dogs with glaucoma often exhibit reduced SOD activity in the aqueous humor and retinal tissues. This decrease limits the capacity to neutralize superoxide radicals effectively, leading to increased oxidative damage. The reduced activity may correlate with disease severity, suggesting that antioxidant defense is compromised in glaucomatous dogs. A reduced level of SOD activity can lead to increased oxidative stress, as excess superoxide radicals are not adequately converted to hydrogen peroxide. This imbalance can lead to a cascade of cellular damage, including lipid peroxidation, protein oxidation, and ultimately apoptosis of RGCs. Elevated markers of oxidative damage, such as MDA, may be observed alongside reduced SOD activity, further substantiating the association with glaucoma [25].

- CAT

CAT primarily converts H_2O_2, a potentially harmful byproduct of cellular metabolism and oxidative stress, into water and oxygen. This reaction helps mitigate oxidative damage within cells, especially in organs such as the eye, where oxidative stress can lead to severe complications like RGC death. In canine glaucoma, elevated IOP leads to increased ROS production, resulting in increased hydrogen peroxide accumulation. CAT efficiently neutralizes H_2O_2, preventing oxidative damage to retinal cells. By maintaining low H_2O_2 levels, CAT protects the retina's delicate cellular structures from oxidative stress-induced apoptosis. Studies have reported that dogs with glaucoma exhibit reduced CAT activity in ocular tissues, elevated IOP, and markers of oxidative stress. A decrease in CAT activity compromises the eye's ability to handle elevated hydrogen peroxide levels, leading to increased oxidative damage and cellular apoptosis, particularly in RGCs. This decline in CAT activity is often associated with the severity of glaucoma, as higher rates of oxidative damage correlate with lower CAT activity [26].

- GPX

GPX is an enzyme that catalyzes the reduction of H_2O_2 and organic hydroperoxides by utilizing GSH as a substrate, resulting in the generation of oxidized glutathione (GSSG) and water. In canine glaucoma, increased IOP correlates with increased ROS production and oxidative stress, leading to hydrogen peroxide accumulation. GPX helps detoxify H_2O_2, protecting RGCs and other ocular tissues from oxidative damage. By effectively reducing H_2O_2 levels, GPX plays a crucial role in preventing cell death and preserving retinal function. Studies have shown that dogs diagnosed with glaucoma exhibit significantly reduced GPX activity in ocular tissues and in the aqueous humor. This reduction correlates with elevated oxidative stress markers, indicating compromised antioxidant defense and potentially exacerbating retinal damage and RGC apoptosis. Low GPX activity may parallel increased markers of oxidative damage, such as MDA, further underscoring its association with glaucoma severity [23].

2.5. Inflammation Biomarkers

Canine glaucoma is a complex disease that presents significant challenges in veterinary ophthalmology, with inflammation playing a key role in the disease's progression. Growing evidence indicates that inflammatory mediators and oxidative stress markers are crucial indicators of the disease's underlying mechanisms. Understanding these markers not only aids in diagnosing glaucoma but also improves our knowledge of the fundamental processes involved, including the interaction between oxidative stress and inflammation.

- Cytokines and Interleukin

Cytokines and interleukins act as critical mediators of inflammation in canine glaucoma, offering insight into the underlying pathophysiological mechanisms and facilitating potential therapeutic interventions. In canine glaucoma, elevated levels of pro-inflammatory cytokines, including interleukin-1 (IL-1), interleukin-6 (IL-6), and TNF-α, have been documented. These cytokines play a pivotal role in recruiting inflammatory cells, including neutrophils and macrophages, to the injury site, thereby worsening the inflammatory response. Dysregulation of these cytokines can lead to sustained inflammation, which is associated with RGC degeneration in glaucoma. Elevated IL-6 levels, for example, have been linked to increased RNFL loss, indicating its potential as a biomarker for disease severity [19]. The mechanism of cytokine involvement includes the activation of retinal microglia and other innate immune cells, which release inflammatory mediators contributing to neurodegeneration. As inflammatory cytokines trigger signaling pathways that induce apoptosis in RGCs, their persistent presence can lead to chronic damage. For instance, IL-1 stimulates MMP production, which contributes to pathological remodeling of the extracellular matrix in the trabecular meshwork, thereby affecting aqueous humor outflow and raising IOP. This interaction between elevated IOP, abnormal cytokine signaling, and inflammation creates a vicious cycle that progressively exacerbates glaucomatous changes in the affected eye [8].

- Matrix metalloproteinases (MMPs)

MMPs play a significant role as biomarkers of inflammation in canine glaucoma, linking inflammation to the neurodegenerative processes that characterize this disease. Glaucoma is associated with neuronal degeneration, particularly in RGCs, a hallmark of the condition [27]. In canine glaucoma, elevated pro-inflammatory proteins, such as MMPs and cytokines, in the aqueous humor have been associated with increased IOP and subsequent RGC damage. MMP-9, a critical ECM remodeling enzyme, is upregulated by elevated IOP and has been shown to contribute to RGC death via oxidative stress and inflammation. Identifying such proteomic markers in the aqueous humor allows for the distinction between normal and glaucomatous states, thus serving diagnostic and prognostic purposes [12]. The mechanisms by which MMPs contribute to neuroinflammation in canine glaucoma can be elucidated through several key pathways. For instance, the activation of microglial cells and astrocytes in response to RGC injury leads to the release of MMPs, facilitating the degradation of the extracellular matrix, thereby influencing both inflammation and neuronal survival [19]. Additionally, canine primary glaucoma is associated with an inflammatory response characterized by increased expression of inflammatory markers, such as MCP-1 and TNF-α. This response has been observed to correlate with the severity of neurodegeneration and increased MMP activity, supporting the hypothesis that these molecules serve as mediators of ocular inflammatory responses [13].

Clinically, the relevance of MMPs as biomarkers extends to their potential for use in diagnostic and therapeutic strategies for glaucoma management. Their quantifiable presence in ocular tissues, such as the aqueous humor, enables the monitoring of disease progression and therapeutic response. Furthermore, anti-inflammatory treatments, including corticosteroids, may have beneficial effects in modulating the inflammatory environment and potentially reducing MMP-triggered damage within the ocular environment, highlighting the therapeutic implications of targeting MMPs [27].

- Glial Biomarkers

Glial biomarkers, such as myelin basic protein (MBP) and S100B, are crucial for understanding the neuroinflammatory processes linked to canine glaucoma. MBP is a structural protein in the myelin sheath surrounding nerve fibers. In canine glaucoma, elevated levels of MBP in the aqueous humor may indicate demyelination and glial disruption in response to neuronal apoptosis and degeneration. MBP can serve as a biomarker for neuroinflammation, suggesting an active inflammatory response in the optic nerve and retinal tissues. Protein S100B is a calcium-binding protein predominantly located in astrocytes and is associated with neuroinflammatory responses. Increased levels of S100B in the cerebrospinal fluid and peripheral areas have been correlated with various neurodegenerative diseases, including glaucoma [21]. In dogs with primary glaucoma, elevated S100B levels in the retina and aqueous humor may indicate astrocyte activation and ongoing neuroinflammatory processes. This might reflect a heightened inflammatory environment that contributes to RGC degeneration. Both MBP and S100B can influence the release of pro-inflammatory cytokines. Dysregulation of these biomarkers may lead to increased RGC apoptosis via inflammatory signaling pathways. For instance, S100B can stimulate TNF-α and other cytokine release from glial cells, promoting a neuroinflammatory environment that exacerbates RGC damage [12].

In glaucomatous canine eyes, abnormal MBP and S100B levels suggest ongoing neuroinflammation and nerve injury. The simultaneous increases in these biomarkers correlate with the progression of the disease, reinforcing their roles as potential indicators of severity [27]. Abnormal MBP and S100B expression may reflect demyelination and a reactive state in glial cells. This reactivity can lead to the loss of normal glial functions, worsening outcomes for RGCs. Elevated S100B levels, in particular, indicate not just inflammation but also stress on astrocytes as they attempt to respond to the neuronal injury, showcasing the dual role of these cells as both protectors and contributors to pathology [8].

- Neuroinflammatory

Neuroinflammation plays a significant role in the development and progression of canine glaucoma, serving as an important inflammatory biomarker. Key proteins, such as glial fibrillary acidic protein (GFAP) and ionised calcium-binding adaptor molecule 1 (IBA1), indicate neuroinflammatory activity in glaucomatous eyes. Their expression reflects the activation of glial cells, which are critical to neuronal health and viability. In response to elevated IOP and oxidative stress, astrocytes and microglia become activated, as evidenced by GFAP upregulation, primarily expressed in astrocytes. GFAP is a reliable biomarker for astrocyte activation, indicating a neuroinflammatory response [16]. Similarly, IBA1 is a marker of microglial activation, crucial for assessing morphological changes in microglia during neuroinflammatory processes [25]. The elevation of neuroinflammatory biomarkers, such as GFAP and IBA1, alongside increased oxidative stress, indicates a decline in RGC health. Studies have shown that as neuroinflammation progresses, GSH levels in RGCs and surrounding glial cells decrease. This decline compromises RGC viability and contributes to the neurodegenerative processes characteristic of glaucoma [13]. Abnormal upregulation of GFAP indicates reactive astrogliosis, a process in which astrocytes proliferate and become hypertrophic in response to injury, releasing inflammatory mediators that can harm surrounding neurons. This offers insight into the severity of the neuroinflammatory response in glaucomatous eyes. Enhanced expression of IBA1 in microglia signifies an active immune response, suggesting that neuroinflammation may play a role in the ongoing degeneration of RGCs [19]. This exacerbates the cycle of inflammation and RGC death, leading to significant visual impairment over time.

3. Conclusions

Canine glaucoma is characterized by elevated IOP that can lead to irreversible optic nerve damage and vision loss. **Clinical markers** are critical in diagnosing glaucoma and monitoring disease progression. Inflammatory markers demonstrate a strong association with RGC death and disease severity. Oxidative stress markers reflect cellular damage and contribute to RGC apoptosis, shedding light on the oxidative pathways involved in glaucoma pathogenesis. Genetic biomarkers provide essential information regarding hereditary predispositions to canine glaucoma. The combination of these factors underscores the complexity of canine glaucoma, wherein clinical markers, inflammatory processes, oxidative stress, and genetic predispositions collectively inform the understanding and diagnosis of this debilitating condition. These biomarkers not only aid in the early detection and monitoring of glaucoma but also offer opportunities to develop targeted therapies to mitigate the disease's progression in canines.

Author Contributions: writing-original draft preparation and editing, A.L.M.N.; writing-review and editing, F.I., T.I. All authors agreed to publish the final version of the manuscript.

Data Availability Statement: The articles used in this review have been appropriately credited and cited for accessibility. The extracted data from chosen articles supporting the findings of this review are presented within the manuscript and are available from the corresponding author upon reasonable request.

Funding: The authors wish to express their gratitude to the Directorate of Research and Innovation Indonesia, through the Riset dan Inovasi untuk Indonesia Maju (RIIM) Program, Vol. 4, No. 24/IV/KS/02/2025 and No. 794/UN1/DITLIT/DitLit/PT/01/03/2025.

Conflicts of Interest: The authors declare no conflicts of interest

References

1. Zăvoi, A.A.; Enache, A.E. Glaucoma in Dogs. *Cluj Vet J* **2021**, *26*, 8-22, doi:10.52331/cvj.v26i3.34.
2. Strom, A.R.; Hässig, M.; Iburg, T.M.; Spiess, B.M. Epidemiology of canine glaucoma presented to University of Zurich from 1995 to 2009. Part 2: secondary glaucoma (217 cases). *Vet Ophthalmol* **2011**, *14*, 127-132, doi:10.1111/j.1463-5224.2010.00854.x.

3. Alghamdi, A.S.A.; Alghamdi, A.I.A.; alahmadi, D.H.; Alkuwaykibi, M.K.G.; Swead, F.A.; Lami, A.I.; Almutairi, N.S.; S.Almutairi, S.; Alanazi, R.F.M.; Aldossari, A.N.; et al. Glaucoma Management Approach: Simple Literature Review. *Arch Pharm Pract* **2019**, *10*, 25-28, doi:10.51847/eqtDHOt5lY.
4. Graham, K.L. Biomarkers of canine glaucoma. Dissertation, The University of Sydney, Sydney, 2019.
5. Beykin, G.; Norcia, A.M.; Srinivasan, V.J.; Dubra, A.; Goldberg, J.L. Discovery and clinical translation of novel glaucoma biomarkers. *Prog Retin Eye Res* **2021**, *80*, 100875, doi:10.1016/j.preteyeres.2020.100875.
6. Gough, A. Dog breed screening for glaucoma prevalence. *VetTimes* 2017.
7. Blanca, P.M.; María Luisa, F.R.; Guadalupe, M.; Fátima, C.L. Oxidative Stress in Canine Diseases: A Comprehensive Review. *Antioxidants (Basel)* **2024**, *13*, doi:10.3390/antiox13111396.
8. Dammak, A.; Huete-Toral, F.; Carpena-Torres, C.; Martin-Gil, A.; Pastrana, C.; Carracedo, G. From Oxidative Stress to Inflammation in the Posterior Ocular Diseases: Diagnosis and Treatment. *Pharmaceutics* **2021**, *13*, doi:10.3390/pharmaceutics13091376.
9. Schellack, N.; Bezuidenhout, S. Glaucoma: a brief review. *S Afr Pharm J* **2015**, *82*, 18-22, doi:doi:10.10520/EJC174862.
10. Hamor, R.E. Clinical Considerations With Glaucoma **2013**. https://vetmed.illinois.edu/wp-content/uploads/2014/04/Glaucoma-Considerations.pdf
11. Kato, K.; Sasaki, N.; Matsunaga, S.; Nishimura, R.; Ogawa, H. Incidence of canine glaucoma with goniodysplasia in Japan: a retrospective study. *J Vet Med Sci* **2006**, *68*, 853-858, doi:10.1292/jvms.68.853.
12. Baudouin, C.; Kolko, M.; Melik-Parsadaniantz, S.; Messmer, E.M. Inflammation in Glaucoma: From the back to the front of the eye, and beyond. *Prog Retin Eye Res* **2021**, *83*, 100916, doi:10.1016/j.preteyeres.2020.100916.
13. Vohra, R.; Tsai, J.C.; Kolko, M. The role of inflammation in the pathogenesis of glaucoma. *Surv Ophthalmol* **2013**, *58*, 311-320, doi:10.1016/j.survophthal.2012.08.010.
14. Izzotti, A.; Bagnis, A.; Saccà, S.C. The role of oxidative stress in glaucoma. *Mutat Res* **2006**, *612*, 105-114, doi:10.1016/j.mrrev.2005.11.001.
15. Raut, S.; Venugopal, S.; Philip, L.; Martin, K.; George, A.; Joy, G. Management of canine glaucoma using a combination of dorzolamide and timolol. *J Vet Anim Sci* **2023**, *54*, doi:10.51966/jvas.2023.54.4.1127-1130.
16. Park, S.A.; Komáromy, A.M. Biomechanics of the optic nerve head and sclera in canine glaucoma: A brief review. *Vet Ophthalmol* **2021**, *24*, 316-325, doi:10.1111/vop.12923.
17. Webb, T.E.R. A review of glaucoma surgical therapy. *Vet Ophthalmol* **2021**, *24 Suppl 1*, 34-38, doi:10.1111/vop.12852.
18. Komáromy, A.M.; Bras, D.; Esson, D.W.; Fellman, R.L.; Grozdanic, S.D.; Kagemann, L.; Miller, P.E.; Moroi, S.E.; Plummer, C.E.; Sapienza, J.S.; et al. The future of canine glaucoma therapy. *Vet Ophthalmol* **2019**, *22*, 726-740, doi:10.1111/vop.12678.
19. Lin, B.; Li, D. The pivotal role of inflammatory factors in glaucoma: a systematic review. *Front Immunol* **2025**, *16*, 1577200, doi:10.3389/fimmu.2025.1577200.
20. Yun, S.; Kang, S.; Kim, Y.; Seo, K. A Retrospective Study of Canine Primary Glaucoma (2011-2020). *J Vet Clin* **2022**, *39*, 162-167, doi:10.17555/jvc.2022.39.4.162.
21. Graham, K.L.; McCowan, C.; White, A. Genetic and Biochemical Biomarkers in Canine Glaucoma. *Vet Pathol* **2017**, *54*, 194-203, doi:10.1177/0300985816666611.
22. Javier, F.; Martinez, H. General on Glaucoma and Oxidative Stress. Comments on Study Design: "Biomarkers of Lipid Peroxidation in the Aqueous Humor of Primary Open-angle Glaucoma Patients". 2017.
23. Hondur, G.; Göktas, E.; Yang, X.; Al-Aswad, L.; Auran, J.D.; Blumberg, D.M.; Cioffi, G.A.; Liebmann, J.M.; Suh, L.H.; Trief, D.; et al. Oxidative Stress-Related Molecular Biomarker Candidates for Glaucoma. *Invest Ophthalmol Vis Sci* **2017**, *58*, 4078-4088, doi:10.1167/iovs.17-22242.
24. Chen, T.; Gionfriddo, J.R.; Tai, P.Y.; Novakowski, A.N.; Alyahya, K.; Madl, J.E. Oxidative stress increases in retinas of dogs in acute glaucoma but not in chronic glaucoma. *Vet Ophthalmol* **2015**, *18*, 261-270, doi:10.1111/vop.12177.
25. Kimura, A.; Namekata, K.; Guo, X.; Noro, T.; Harada, C.; Harada, T. Targeting Oxidative Stress for Treatment of Glaucoma and Optic Neuritis. *Oxid Med Cell Longev* **2017**, *2017*, 2817252, doi:10.1155/2017/2817252.
26. Dammak, A.; Sanchez Naves, J.; Huete-Toral, F.; Carracedo, G. New Biomarker Combination Related to Oxidative Stress and Inflammation in Primary Open-Angle Glaucoma. *Life (Basel)* **2023**, *13*, doi:10.3390/life13071455.
27. Sebbag, L.; Pe'er, O. Role of Inflammation in Canine Primary Glaucoma. *Animals (Basel)* **2023**, *14*, doi:10.3390/ani14010110.